ELECTROSPINNING APPLICATIONS IN MECHANOCHEMISTRY AND MULTI-FUNCTIONAL HYDROGEL MATERIALS

BY

AUSTIN N. PICKETT

THESIS

Submitted in partial fulfillment of the requirements
for the degree of Master of Science in Materials Science and Engineering
in the Graduate College of the
University of Illinois at Urbana-Champaign, 2012

Urbana, Illinois

Adviser:

Professor Paul V. Braun

Report Documentation Page

Form Approved
OMB No. 0704-0188

1. REPORT DATE	2. REPORT TYPE	3. DATES COVERED
2012		**00-00-2012 to 00-00-2012**

4. TITLE AND SUBTITLE	5a. CONTRACT NUMBER
Electrospinning Applications in Mechanochemistry and Multi-Functional Hydrogel Materials	5b. GRANT NUMBER
	5c. PROGRAM ELEMENT NUMBER
6. AUTHOR(S)	5d. PROJECT NUMBER
	5e. TASK NUMBER
	5f. WORK UNIT NUMBER
7. PERFORMING ORGANIZATION NAME(S) AND ADDRESS(ES) **University of Illinois at Urbana-Champaign,Urbana,IL,61801**	8. PERFORMING ORGANIZATION REPORT NUMBER
9. SPONSORING/MONITORING AGENCY NAME(S) AND ADDRESS(ES)	10. SPONSOR/MONITOR'S ACRONYM(S)
	11. SPONSOR/MONITOR'S REPORT NUMBER(S)

12. DISTRIBUTION/AVAILABILITY STATEMENT
Approved for public release; distribution unlimited

13. SUPPLEMENTARY NOTES

14. ABSTRACT

Mechanochemistry is the use of mechanical force to perform chemical reactions and has the potential to bring self-healing functionality to the molecular level. The mechanically induced reactions can become productive when stress-sensitive molecules, or mechanophores, are incorporated into materials. One mechanophore that has been heavily investigated is spiropyran a molecule that exhibits a color change when activated, although large strains are required to achieve this activation in elastomeric materials. In addition to color change, the activation of nonpolar spiropyran also results in the formation of a polar species. Electrospinning, a process used to produce very small fibers, has the potential to be used in a number of applications in mechanochemistry. These very small fibers have been shown to possess high molecular orientation, which is a result of the high longitudinal strains imparted to the fibers during their formation. This thesis investigated if low-strain activation of spiropyran could be achieved with the high degree of molecular orientation in electrospun nanofibers. It was also determined whether the high strains during electrospinning could be used to activate gem-dibromocyclopropane, an irreversible mechanophore. Finally, it was explored if the nonpolar-to-polar transition of spiropyran could be used to induce swelling in hydrogels.

15. SUBJECT TERMS

16. SECURITY CLASSIFICATION OF:			17. LIMITATION OF ABSTRACT	18. NUMBER OF PAGES	19a. NAME OF RESPONSIBLE PERSON
a. REPORT **unclassified**	b. ABSTRACT **unclassified**	c. THIS PAGE **unclassified**	**Same as Report (SAR)**	**71**	

ABSTRACT

Mechanochemistry is the use of mechanical force to perform chemical reactions and has the potential to bring self-healing functionality to the molecular level. The mechanically induced reactions can become productive when stress-sensitive molecules, or mechanophores, are incorporated into materials. One mechanophore that has been heavily investigated is spiropyran, a molecule that exhibits a color change when activated, although large strains are required to achieve this activation in elastomeric materials. In addition to color change, the activation of nonpolar spiropyran also results in the formation of a polar species.

Electrospinning, a process used to produce very small fibers, has the potential to be used in a number of applications in mechanochemistry. These very small fibers have been shown to possess high molecular orientation, which is a result of the high longitudinal strains imparted to the fibers during their formation.

This thesis investigated if low-strain activation of spiropyran could be achieved with the high degree of molecular orientation in electrospun nanofibers. It was also determined whether the high strains during electrospinning could be used to activate *gem*-dibromocyclopropane, an irreversible mechanophore. Finally, it was explored if the nonpolar-to-polar transition of spiropyran could be used to induce swelling in hydrogels.

ACKNOWLEDGEMENTS

Any and all success that I have experienced in my life can be directly attributed to my parents. Whether helping me with grade school homework or the construction of my ill-conceived high school science project, they have always been there offering physical and emotional support, wake-up calls (both in a literal and figurative sense), and a soft landing should I falter. I would also like to thank my brother, Adam. He was always bigger and stronger than I in our youth, and I cannot help but believe, on an unconscious level, that I was driven to science in hopes of eventually gaining the upper hand.

I would like to express sincere gratitude to my research advisor, Professor Paul V. Braun. He has shown more patience and understanding than I probably deserved while providing invaluable guidance, helpful suggestions, and a number of professional and scientific opportunities.

I would like to acknowledge a number of my colleagues including Kevin Arpin, Dr. Aaron Jackson, Dr. Mark Losego, Dr. Jeong-Ho Park, Ariane Vartanian, Corissa Lee, Brett Beiermann, Amanda Jones, Dr. Douglas Davis, Preston May, and Ashley Black-Ramirez. There are many other members of the Braun and AMS groups that I may not have collaborated with directly, but their input was appreciated all the same.

I would also like to thank the many friends that I have made since beginning graduate school. I was fortunate enough to join a very welcoming department full of social people who have made this an enjoyable and rewarding experience.

Finally, I would like to thank the facilities of the Beckman Institute and Materials Research Laboratory and the Army Research Office MURI (Grant W011NF-07-1-0409) for financial support.

TABLE OF CONTENTS

CHAPTER ONE: INTRODUCTION 1
1.1 Mechanochemistry 1
1.2 Spiropyran as a Mechanophore 4
1.3 *gem*-Dihalocyclopropane Mechanophores 7
1.4 Electrospinning 8
1.5 References 12

CHAPTER TWO: ELECTROSPINNING OF SPIROPYRAN-POLYURETHANE 16
2.1 Motivation 16
2.2 Electrospinning of Isotropic Fiber Mats 17
2.3 Electrospinning of Aligned Fiber Mats 20
2.4 Summary 30
2.5 References 31

CHAPTER THREE: ELECTROSPINNING OF *gem*-DIBROMOCYCLOPROPANE MECHANOPHORES 32
3.1 Introduction and Motivation 32
3.2 Experimental 36
3.3 Analysis of Electrospun *g*DBC Fibers 38
3.4 Additional Experiments 42
3.5 Summary 43
3.6 References 43

CHAPTER FOUR: MULTI-FUNCTIONAL SPIROPYRAN-CONTAINING HYDROGELS 46
4.1 Introduction and Motivation 46
4.2 Spiropyran-HEMA Hydrogels 49
4.3 Spiropyran-NIPAM Hydrogels 53
4.4 Spiropyran-PMMA Hydrogels 56
4.5 P(MMA:NIPAM) and P(MMA:HEMA) Copolymers 58
4.6 Summary 60
4.7 References 61

CHAPTER FIVE: CONCLUSIONS AND FUTURE WORK 63
5.1 Electrospinning of Spiropyran-Polyurethane 63
5.2 Electrospinning of *gem*-Dibromocyclopropane Mechanophores 64
5.3 Multi-Functional Spiropyran-Containing Hydrogels 65
5.4 References 67

CHAPTER ONE

INTRODUCTION

1.1 Mechanochemistry

The original motivation behind the field of mechanochemistry was to transition self-healing ability from the microscopic world of cracks and capsules[1, 2] to the nanoscopic molecular level. In a broad sense, mechanochemistry can be defined as the use of mechanical force to produce a chemical change in a substance.

Until recently, the term mechanochemistry was predominately used in the inorganic and biological disciplines. In fact, the change in appearance and, in some cases, chemical reactions of salts and metal oxides as a result of mechanical pressure were first reported by M. Carry Lea in 1893.[3] More recently, a variety of carbides,[4] silicides,[5] and pure metals[6] have been synthesized by ball milling of their respective powders at room temperature. In biology, studies have typically focused on the mechanically induced activity of components such as enzymes,[7] muscle fibers,[8] and cell membranes.[9]

In the last decade, however, mechanochemistry has been an area of intense research in the field of polymer science. It has been well-established that polymer chains, when exposed to stress, respond by the breakage of a bond along the backbone, or chain scission.[10, 11] This usually occurs at a weakened bond or near the middle of the chain where ultrasound-induced shear forces are the strongest.[12, 13] However, the incorporation of a stress-sensitive molecule, or mechanophore, can result in a productive chemical reaction before chain scission occurs.

One of the first such mechanophores was benzocyclobutene, developed by Hickenboth and coworkers (**Figure 1.1a)**.[14] In addition to mechanical stress, the mechanophore could be

activated by light and heat; however, these two excitation methods produced a mixture of isomer products (E,E or E,Z) depending on which mechanophore (*cis* or *trans*) was used. Conversely, when exposed to mechanical stress, both *cis* and *trans* mechanophores yielded a single product, the E,E-isomer (Figure 1.1b).

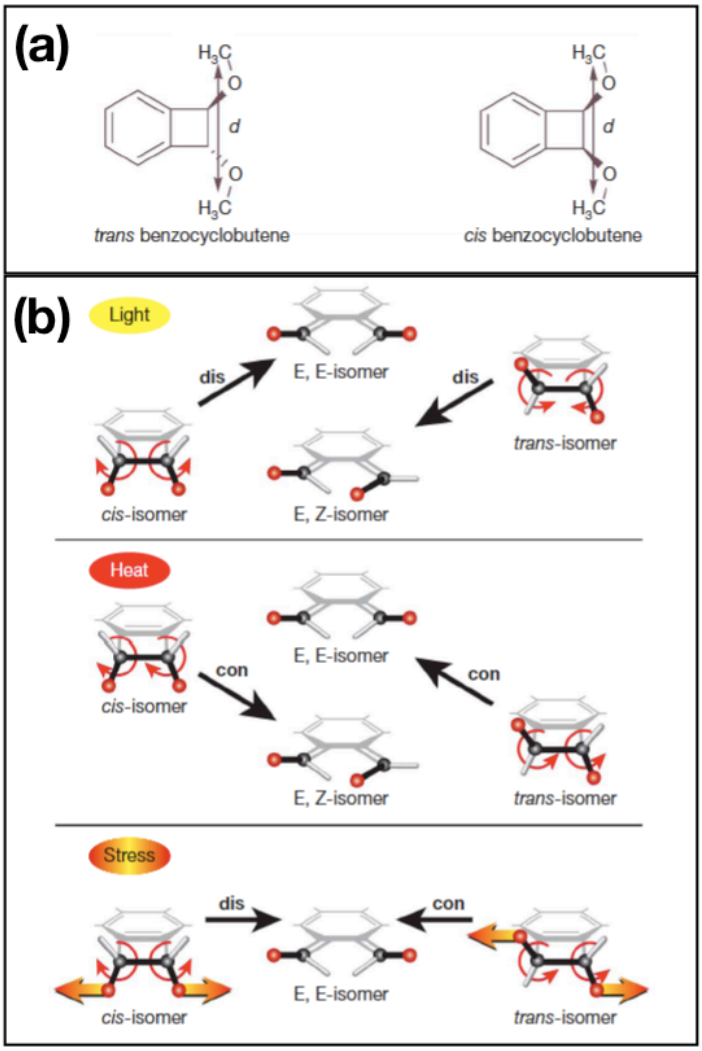

Figure 1.1. (a) *cis*- and *trans*-Benzycyclobutene mechanphore (without polymer chains attached). (b) The pathways of thermal, mechanical, and photo-induced activation of the *cis* and *trans* isomers. Adapted from Hickenboth *et al.*[14]

The phenomenon that mechanical stress could produce unique species that could not be produced by heat, light, or other means resulted in a dramatic increase in research regarding this application of mechanochemistry. Lenhardt *et al.*[15] were able to achieve mechanical isomerization of *gem*-difluorocyclopropanes, which resulted in the formation of thermodynamically disfavored *cis*-products (**Figure 1.2**). In contrast, the major product of thermal isomerization was the lower-energy *trans*-product. Klukovich and coworkers[16] used ultrasound to generate trifluorovinyl ethers from perfluorocyclobutanes via a formal [2 +2] cycloreversion **(Figure 1.3**). This process not only produced a different species than thermolysis, but the reactive trifluorovinyl ethers could then be thermally treated to regenerate the original polymer.

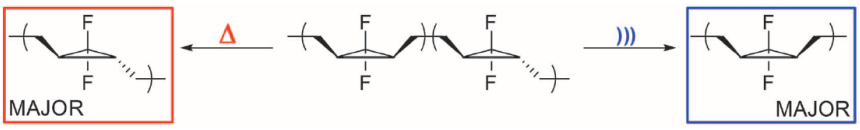

Figure 1.2. Major products of thermal and mechanical isomerization of *gem*-difluorocyclopropanes. Adapted from Lenhardt *et al.*[15]

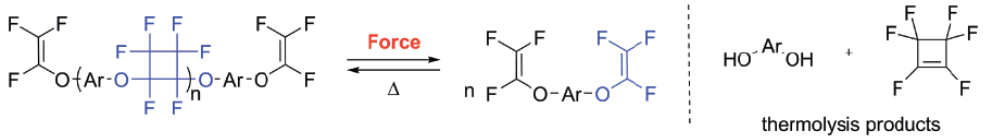

Figure 1.3. Mechanical and thermal products of perfluorocyclobutanes. Mechanical products could be thermally treated to reform original polymer. Adapted from Wiggins *et al.*[17]

Piermattei *et al.*[18] have used mechanochemistry to achieve the activation of heterocyclic catalysts. The catalyst complexes, a single metal center (silver or ruthenium) chelated by two N-

heterocyclic carbenes with polymer chains attached, remained latent until sonication cleaved the metal-ligand bond. The now-activated catalyst could then participate in transesterification, ring-closing metathesis, and ring-opening metathesis polymerization reactions (**Figure 1.4**). Although yields were much lower than traditional catalysts, most likely due to rapid catalyst degradation, mechanically activated catalysis has significant potential in the field of self-healing materials.

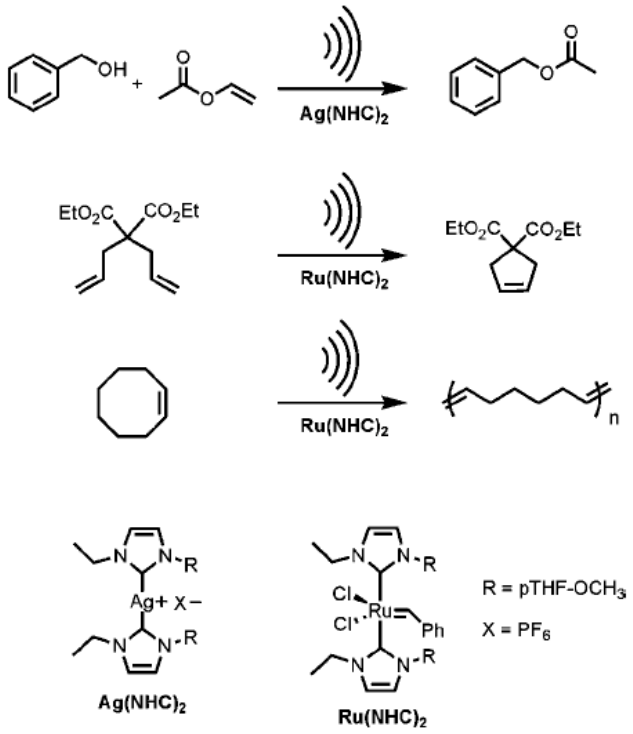

Figure 1.4. Mechanochemical activation of a catalytic transesterification, ring-closing metathesis, and ring-opening metathesis polymerization. Adapted from Caruso *et al.*[13]

1.2 Spiropyran as a Mechanophore

Mechanochemistry has also experienced significant research in the area of damage detection through the use of the spiropyran mechanophore.[19-23] Prior to mechanochemical studies, the small molecule was well known for its ability to transition from a colorless

spiropyran (SP) form to a highly colored merocyanine (MC) form (**Figure 1.5a**), and this transformation can be caused by a number of conditions including exposure to ultraviolet radiation, increased temperatures, and polar solvents.[24]

The first mechanochemical activation of a spiropyran-containing polymer was accomplished by Potisek *et al*.[23] This was achieved by exposing the dissolved polymer to ultrasound, and the solution gradually transitioned from colorless to pink. The color change was accompanied by an increase in the characteristic absorption peak of the merocyanine form. The end-functionalized control samples were not able to experience mechanical force and did not show activation (Figure 1.5b).

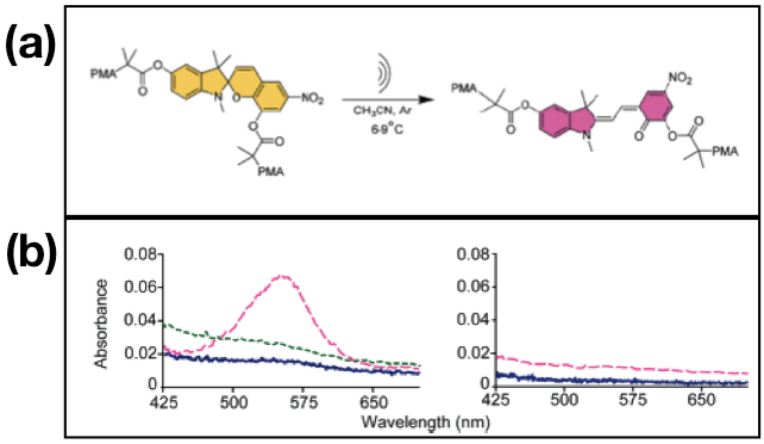

Figure 1.5. (a) Spiropyran-merocyanine transition caused by ultrasonic radiation. (b) UV spectrums of PMA-SP-PMA (left) and end-functionalized PMA-SP control (right). Spectrum before sonication (blue trace), after 18 minutes pulsed sonication (dashed pink trace), and after 40 minutes exposure to ambient light (dotted green trace). Adapted from Potisek *et al*.[23]

The first mechanical activation of a spiropyran-polymer in the solid state was accomplished by Davis and coworkers.[21] Spiropryan mechanophores were incorporated in two polymeric materials, poly(methyl acrylate) (PMA) and poly(methyl methacrylate) (PMMA). SP-containing PMA, a highly elastomeric polymer, was formed into "dog bone" structures and

loaded under tensile stress. The necks of the dog bones turned bright red under stress, while control samples experienced no color change (**Figure 1.6**). SP-containing PMMA, a glassy polymer, was formed into beads and loaded under compressive stress. As the bead was compressed, tensile stresses developed within the polymer and resulted in a color change in SP-containing samples while control samples showed no color change.

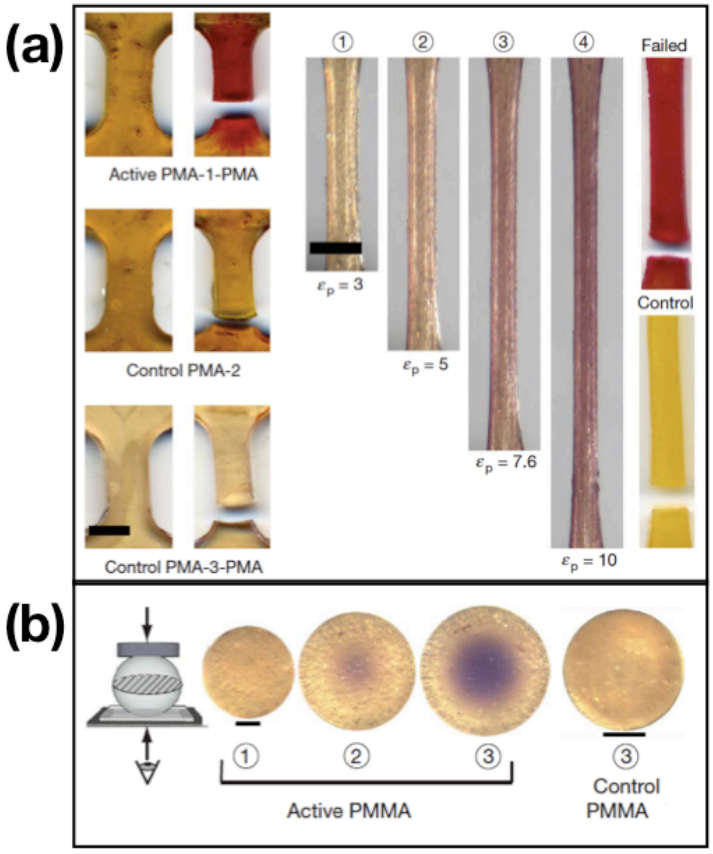

Figure 1.6. (a) Response of SP-containing (active) and control PMA dog bones under tensile loading. (b) Response of SP-containing (active) and control PMMA beads under compressive stress. Adapted from Davis *et al.*[21]

Spiropyran was later incorporated into bulk polyurethane to investigate the thermodynamics and kinetics of activation.[22] Polyurethane provided a more attractive platform for this type of study given its mechanical toughness, elasticity, and low glass transition temperature. When a polyurethane dog bone was stretched, a bright purple color change was

produced (**Figure 1.7**). As with the spiropyran-containing PMA, removal of the stressor caused the higher-energy merocyanine form to slowly revert back to the energetically-favored spiropyran form. As such, the color caused by mechanophore activation slowly disappeared. When the load was maintained on the sample, however, there was no significant decrease in color, indicating mechanical force altered the potential energy surface of the spiropyran-merocyanine interconversion.

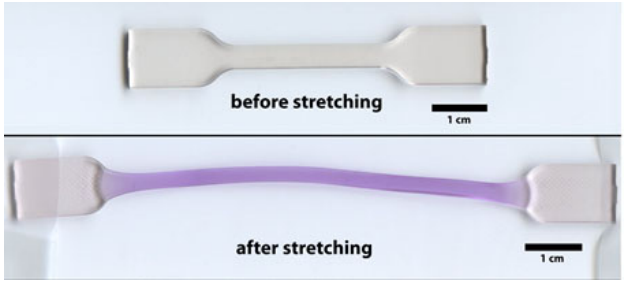

Figure 1.7. SP-polyurethane dog bone before and after stretching.

1.3 *gem*-Dihalocyclopropane Mechanophores

Another series of mechanophores that have been extensively investigated are the *gem*-dihalocyclopropanes of the Stephen L. Craig group (**Figure 1.8**).[15, 25-28] Mechanophores of this type have the disadvantage that activation is not able to be detected visibly, like spiropyran, and requires NMR spectroscopy; although, NMR is a much more sensitive detection technique than optical color change. One advantage of the mechanophore is that activation is irreversible, which allows for activation studies that would not be possible with reversible spiropyran.

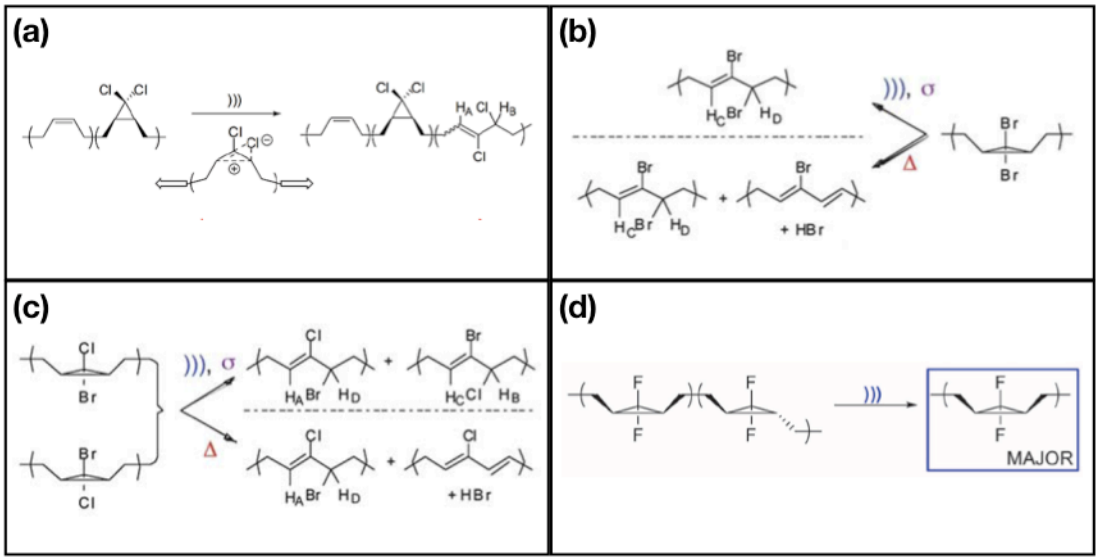

Figure 1.8. *gem*-Dihalocyclopropanes. (a) -chloro,[25] (b) –bromo, (c) -bromochloro,[27] and (d) -fluorocyclopropanes.[15]

1.4 Electrospinning

1.4.1 History and Fundamentals

Electrospinning is a simple and effective technique for producing fibers ranging from tens of nanometers to micrometers. Although the effects of electric fields on fluids have been studied for hundreds of years, the process of electrospinning was not patented until 1934 by Formhals.[29] The technique was utilized and researched very little, however, until the mid-1990s when Doshi and Reneker demonstrated the fabrication of thin fibers from a broad range of organic polymers.[30] Since then, there has been an exponential growth of research in both the theory and applications of electrospinning. Although electrospinning has been primarily used for the fabrication of fibers from synthetic organic polymers, it can also be used for biological molecules[31, 32] and ceramic sol precursors.[33, 34]

A schematic for a basic electrospinning apparatus is shown in **Figure 1.9**. A polymer fluid is fed at a constant rate, usually via syringe pump, through a metallic needle or capillary. A

high voltage, usually on the order of 5-30 kV, is applied to the needle. The emerging polymer solution forms a cone, commonly referred to as a Taylor cone,[35] and a fluid jet is ejected and accelerated toward the grounded collector. As it travels to the collector, the solvent evaporates and the fiber begins thinning and whipping as a result of electrostatic bending instability. The flight of the fluid jet has been studied quite extensively and it involves complex electro-fluid-mechanical dynamics.[36-39] The collected fibers usually contain very little, if any, solvent and can vary in size depending on the electrospinning conditions used.

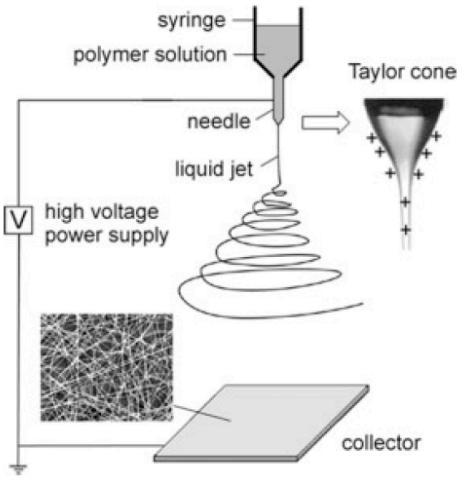

Figure 1.9. Schematic of the basic setup for electrospinning. Insets show micrograph of a nonwoven fiber mat and drawing of electrified Taylor cone. Adapted from Li and Xia.[40]

1.4.2 Molecular Orientation in Electrospun Nanofibers

In addition to producing fibers with diameters as small as tens of nanometers, electrospinning has also been shown to produce nanofibers that have a significant degree of polymer chain alignment, or molecular orientation, in the direction of the fiber.[41-45] Fennessey and Farris electrospun polyacrylonitrile fibers onto a rotating collector at various speeds.[41]

Through infrared dichroism measurements, the fibers were determined to possess a significant degree of molecular orientation and this was attributed to the drawing of the fibers as they landed on the rotating substrate. Yee and coworkers later determined, however, that molecular orientation was caused by Coulombic forces rather than the mechanical and shear forces imparted by the rotating collector.[42] This suggests that, with the proper electrospinning conditions, molecular orientation is inherent to electrospun nanofibers. Naraghi *et al*.[45] used MEMS devices to mechanically test individual polyacrylonitrile nanofibers (**Figure 1.10**). The high elastic moduli and yield strengths of small diameter fibers fabricated at long electrospinning distances suggested a substantial degree of molecular orientation, and this was confirmed with polarized FTIR spectroscopy and wide angle x-ray diffraction.

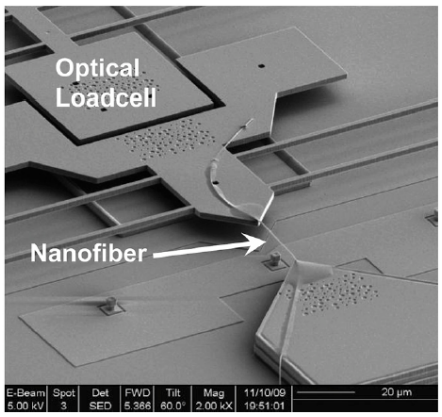

Figure 1.10. Polyacrylonitrile nanofiber mounted on MEMS testing device. Adapted from Naraghi *et al*.[45]

1.4.3 Electrospinning of Aligned Fibers

The fabrication of aligned fibers is of critical importance for a number of applications, including mechanical testing[44] and guiding the growth of specific tissues in tissue engineering.[46] Currently, there are a number of different methods to align electrospun fibers during the

electrospinning process. One of the most common methods to achieve aligned fibers is by electrospinning onto a rotating collector.[47, 48] The direction of rotation can be either perpendicular or parallel to the propagation direction of the electrospinning jet (**Figure 1.11**). The advantage of this system is that fairly thick fiber mats can be collected. Another method is to use an array of conductive substrates (**Figure 1.12**) instead of one large, homogeneous collector.[49] Although the electrode array is easier to setup than the rotating collector, substantial fiber mats cannot be collected as the thickening fiber mat begins to repel newly formed fibers and there is no mechanical rotation to continue to impart alignment.

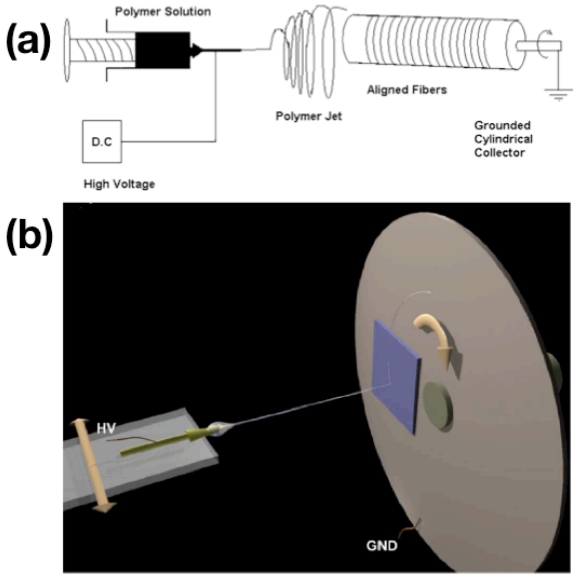

Figure 1.11. Collection of aligned fibers with collection rotation (a) parallel and (b) perpendicular to electrospinning jet. Adapted from (a) Thomas *et al*.[50] and (b) Bellan *et al*.[47]

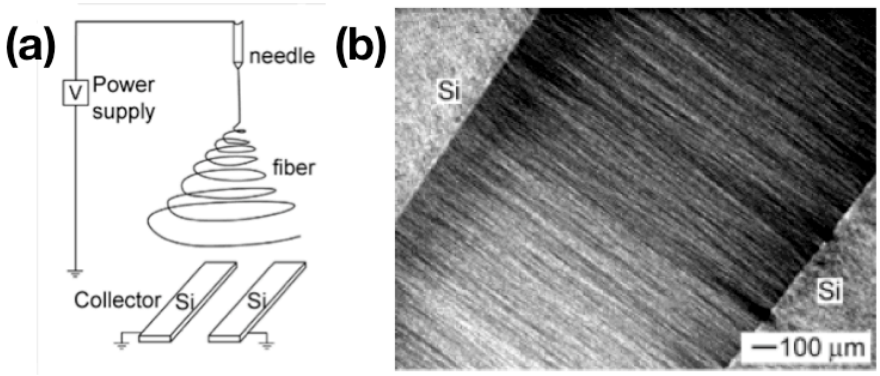

Figure 1.12. (a) Schematic of electrospinning onto electrode array and (b) micrograph of aligned fibers suspended across the electrode gap. Adapted from Li *et al*.[49]

1.5 References

1. Jackson, A. C.; Bartelt, J. A.; Marczewski, K.; Sottos, N. R.; Braun, P. V., *Macromolecular Rapid Communications* **2010,** *32* (1), 82-87.

2. White, S. R.; Sottos, N. R.; Geubelle, P. H.; Moore, J. S.; Kessler, M. R.; Sriram, S. R.; Brown, E. N.; Viswanathan, S., *Nature* **2001,** *409* (6822), 794-797.

3. Lea, M. C., *Philosophical Magazine Series 5* **1893,** *36* (221), 351-354.

4. Matteazzi, P.; Le Caër, G., *Journal of the American Ceramic Society* **1991,** *74* (6), 1382-1390.

5. Matteazzi, P.; Basset, D.; Miani, F.; Le Caër, G., *Nanostructured Materials* **1993,** *2* (3), 217-229.

6. McCormick, P. G., *Mater. Trans. Jpn. Inst. Met.* **1995,** *36* (2), 161-169.

7. Liao, J.-C.; Jeong, Y.-J.; Kim, D.-E.; Patel, S. S.; Oster, G., *Journal of Molecular Biology* **2005,** *350* (3), 452-475.

8. Girard, K. D.; Kuo, S. C.; Robinson, D. N., *Proceedings of the National Academy of Sciences of the United States of America* **2006,** *103* (7), 2103-2108.

9. Liu, J.; Sun, Y.; Drubin, D. G.; Oster, G. F., *PLoS Biol* **2009,** *7* (9), e1000204.

10. Suslick, K. S.; Price, G. J., *Annu. Rev. Mater. Sci.* **1999,** *29*, 295-326.

11. Koda, S.; Mori, H.; Matsumoto, K.; Nomura, H., *Polymer* **1994,** *35* (1), 30-33.

12. Berkowski, K. L.; Potisek, S. L.; Hickenboth, C. R.; Moore, J. S., *Macromolecules* **2005,** *38* (22), 8975-8978.

13. Caruso, M. M.; Davis, D. A.; Shen, Q.; Odom, S. A.; Sottos, N. R.; White, S. R.; Moore, J. S., *Chemical Reviews* **2009,** *109* (11), 5755-5798.

14. Hickenboth, C. R.; Moore, J. S.; White, S. R.; Sottos, N. R.; Baudry, J.; Wilson, S. R., *Nature* **2007,** *446* (7134), 423-7.

15. Lenhardt, J. M.; Ong, M. T.; Choe, R.; Evenhuis, C. R.; Martinez, T. J.; Craig, S. L., *Science* **2010,** *329* (5995), 1057-1060.

16. Klukovich, H. M.; Kean, Z. S.; Iacono, S. T.; Craig, S. L., *Journal of the American Chemical Society* **2011,** *133* (44), 17882-17888.

17. Wiggins, K. M.; Brantley, J. N.; Bielawski, C. W., *ACS Macro Letters* **2012**, 623-626.

18. Piermattei, A.; Karthikeyan, S.; Sijbesma, R. P., *Nat Chem* **2009,** *1* (2), 133-137.

19. Beiermann, B. A.; Davis, D. A.; Kramer, S. L. B.; Moore, J. S.; Sottos, N. R.; White, S. R., *Journal of Materials Chemistry* **2011,** *21* (23), 8443-8447.

20. Beiermann, B. A.; Kramer, S. L. B.; Moore, J. S.; White, S. R.; Sottos, N. R., *ACS Macro Letters* **2012,** *1* (1), 163-166.

21. Davis, D. A.; Hamilton, A.; Yang, J.; Cremar, L. D.; Van Gough, D.; Potisek, S. L.; Ong, M. T.; Braun, P. V.; Martinez, T. J.; White, S. R.; Moore, J. S.; Sottos, N. R., *Nature* **2009,** *459* (7243), 68-72.

22. Lee, C. K.; Davis, D. A.; White, S. R.; Moore, J. S.; Sottos, N. R.; Braun, P. V., *Journal of the American Chemical Society* **2010,** *132* (45), 16107-16111.

23. Potisek, S. L.; Davis, D. A.; Sottos, N. R.; White, S. R.; Moore, J. S., *J. Am. Chem. Soc.* **2007,** *129* (45), 13808-13809.

24. Minkin, V. I., *Chemical Reviews* **2004,** *104* (5), 2751-2776.

25. Lenhardt, J. M.; Black, A. L.; Craig, S. L., *Journal of the American Chemical Society* **2009,** *131* (31), 10818-10819.

26. Wu, D.; Lenhardt, J. M.; Black, A. L.; Akhremitchev, B. B.; Craig, S. L., *Journal of the American Chemical Society* **2010,** *132* (45), 15936-15938.

27. Lenhardt, J. M.; Black, A. L.; Beiermann, B. A.; Steinberg, B. D.; Rahman, F.; Samborski, T.; Elsakr, J.; Moore, J. S.; Sottos, N. R.; Craig, S. L., *Journal of Materials Chemistry* **2011,** *21* (23), 8454-8459.

28. Black, A. L.; Orlicki, J. A.; Craig, S. L., *Journal of Materials Chemistry* **2011,** *21* (23), 8460-8465.

29. Formhals, A. Process and apparatus for preparing artificial threads. 1,975,504, 1934.

30. Doshi, J.; Reneker, D. H., *Journal of Electrostatics* **1995,** *35* (2,Äì3), 151-160.

31. Fang, X.; Reneker, D. H., *Journal of Macromolecular Science, Part B* **1997,** *36* (2), 169-173.

32. Takahashi, T.; Taniguchi, M.; Kawai, T., *Jpn. J. Appl. Phys. Part 2 - Lett. Express Lett.* **2005,** *44* (24-27), L860-L862.

33. Wang, Y.; J. Santiago-Avilés, J., *Nanotechnology* **2004,** *15* (1), 32.

34. Larsen, G.; Velarde-Ortiz, R.; Minchow, K.; Barrero, A.; Loscertales, I. G., *Journal of the American Chemical Society* **2003,** *125* (5), 1154-1155.

35. Taylor, G., *Proceedings of the Royal Society of London. Series A. Mathematical and Physical Sciences* **1964,** *280* (1382), 383-397.

36. Han, T.; Yarin, A. L.; Reneker, D. H., *Polymer* **2008,** *49* (6), 1651-1658.

37. Reneker, D. H.; Yarin, A. L.; Fong, H.; Koombhongse, S., *J. Appl. Phys.* **2000,** *87* (9), 4531-4547.

38. Fernandez de la Mora, J., *Annual Review of Fluid Mechanics* **2006,** *39* (1), 217-243.

39. Feng, J. J., *Journal of Non-Newtonian Fluid Mechanics* **2003,** *116* (1), 55-70.

40. Li, D.; Xia, Y., *Advanced Materials* **2004,** *16* (14), 1151-1170.

41. Fennessey, S. F.; Farris, R. J., *Polymer* **2004,** *45* (12), 4217-4225.

42. Yee, W. A.; Kotaki, M.; Liu, Y.; Lu, X., *Polymer* **2007,** *48* (2), 512-521.

43. Kakade, M. V.; Givens, S.; Gardner, K.; Lee, K. H.; Chase, D. B.; Rabolt, J. F., *Journal of the American Chemical Society* **2007,** *129* (10), 2777-2782.

44. Pedicini, A.; Farris, R. J., *Polymer* **2003,** *44* (22), 6857-6862.

45. Naraghi, M.; Arshad, S. N.; Chasiotis, I., *Polymer* **2011,** *52* (7), 1612-1618.

46. Yang, F.; Murugan, R.; Wang, S.; Ramakrishna, S., *Biomaterials* **2005,** *26* (15), 2603-2610.

47. Bellan, L. M.; Craighead, H. G., *J. Manuf. Sci. Eng.* **2009,** *131* (3), 34001.

48. Teo, W. E.; Ramakrishna, S., *Nanotechnology* **2006,** *17* (14), R89.

49. Li, D.; Wang, Y.; Xia, Y., *Nano Letters* **2003,** *3* (8), 1167-1171.

50. Thomas, V.; Jose, M. V.; Chowdhury, S.; Sullivan, J. F.; Dean, D. R.; Vohra, Y. K., *Journal of Biomaterials Science, Polymer Edition* **2006,** *17* (9), 969-984.

CHAPTER TWO

ELECTROSPINNING OF SPIROPYRAN-POLYURETHANE

2.1 Motivation

One of the primary drawbacks to incorporating a mechanophore into a highly elastomeric material such as polyurethane is that significantly high strains are required for activation. These strains are high enough that they would not be useful for damage detection in a real-world application as the change in physical dimensions of the material would be noticed before the color or fluorescence change caused by the spiropyran-merocyanine transition. Therefore, a mechanophore-containing polymer needs to be prepared, either through processing or novel polymer synthesis, that activates at realistic strains (less than a few percent).

Beiermann *et al.* have investigated the role of mechanophore orientation and its relationship to mechanophore activation.[1] The orientation of the mechanophore molecule can be generally related to the orientation of the attached polymer chains. It was determined that those spiropyran molecules, and thus the polymer chains, oriented in the direction of the applied strain activate prior to those oriented in the perpendicular direction.

Electrospinning has been previously used to produce polyurethane nanofibers.[2-6] Work by Pedicini *et al.*[7] investigated the mechanical properties of electrospun polyurethane mats. These mats had significantly different mechanical properties than bulk polyurethane and this was attributed to a high degree of molecular orientation within the nanofibers. To fully take advantage of the polymer chain orientation required the nanofibers themselves to possess a general alignment within mat, as an isotropic nanofiber mat would simply behave like the bulk sample.

This research investigated if low-strain mechanophore activation can be achieved by producing spiropyran-polyurethane nanofibers, with significant molecular orientation, by electrospinning. This approach is preferential to choosing an entirely new polymer as it uses a system that has already been developed and can be synthesized with consistent results.

2.2 Electrospinning of Isotropic Fiber Mats

2.2.1 Sample Preparation

The synthetic methods for the dihydroxyspiropyran mechanophore, prepared by Doug Davis, and the spiropyran-polyurethane (SP-PU) dog bones, prepared by Corissa Lee, have been reported previously.[8] The result of the process was a slightly purple-hued dog bone, seen in **Figure 2.1**. Either a portion or a complete dog bone was taken and cut into small pieces, usually weighing 10-20 mgs each. This was done to aid in the dissolution of the polymer as allowing it to remain in large pieces usually resulted in incomplete dissolution and/or solution inhomogeneities. A 1:1 THF/DMF (w/w) solution was prepared. The small pieces of polymer were added to the solution to create polymer solutions ranging from 7-15 wt%. The mixture was heated to 40°C and magnetically stirred for a period of 24 hours. After complete dissolution, the viscous solution was allowed to cool to room temperature and then transferred to a 10-mL syringe fitted with a 22-gauge hypodermic needle. The beveled needle tip had been previously ground flat using a bench grinder.

Figure 2.1. Image of SP-PU dog bone product (scale bar = 1cm).[8]

2.2.2 Electrospinning Parameters

The polymer solution was fed at a constant rate via a syringe pump (KDScientific) that was suspended 9 cm above a grounded copper wire mesh with a diameter of 10 cm. The feed rate was fixed at 5.5 μL/min and the metallic needle was connected to a 30 kV high-voltage power supply (RHR30PN10, Spellman). Typical electrospinning voltages ranged from 5-10 kV. To collect fibers, a 1 square-inch piece of silicon wafer (n-type, phosphorus) was placed on the copper wire grid.

2.2.3 Analysis of Nanofiber Formation

A Hitachi S-4700 high-resolution scanning electron microscope (SEM) was used to inspect nanofiber formation on wafers. Prior to SEM, the nanofibers were sputtered with a thin layer of Au/Pd.

2.2.3.1 7-wt% SP-PU Solution

Initial electrospinning attempts were performed with a 7-wt% polymer solution. However, the viscosity of the solution was too low to allow for significant fiber formation. Instead, electrospraying occurred which is evident by the high populations of small droplets on the surface of the silicon wafer (**Figure 2.2a**). Upon closer inspection of the few fibers that did form, the wetting of the fibers on the wafer surface further indicates that too much solvent was present in the electrospinning solution (**Figure 2.2b**).

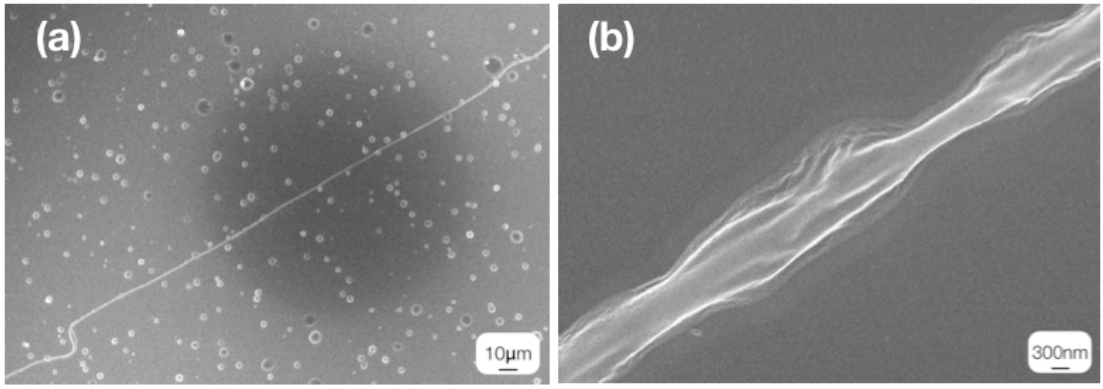

Figure 2.2. (a) Micrograph of electrosprayed SP-PU droplets and a single nanofiber. (b) Wetted nanofiber on silicon, indicating the presence of excess solvent within fibers.

2.2.3.2 10-wt% SP-PU Solution

Given the problems that arose when using the 7-wt% solution, a higher percentage SP-PU solution was prepared. This higher viscosity solution allowed for sustained Taylor cone formation, which resulted in substantial nanofiber mats. Furthermore, the nanofibers appeared to be cylindrical in shape and had none of the wetting issues seen previously (**Figure 2.3**).

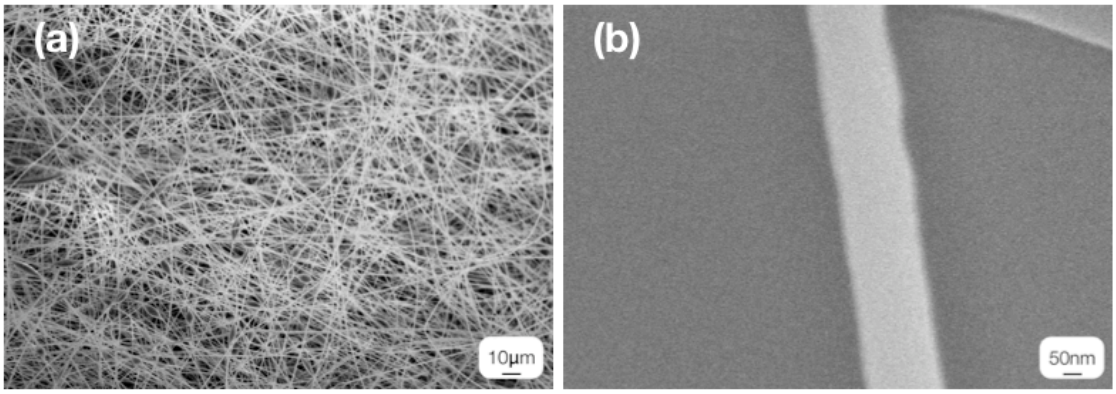

Figure 2.3. (a) Micrograph of thick SP-PU nanofiber mat and (b) cylindrical SP-PU nanofiber.

2.2.3.3 15-wt% SP-PU Solution

A 15-wt% solution was prepared to determine if a higher concentration would yield even better results. However, the solubility of the SP-PU dog bones was low enough that weight-percents of this magnitude yielded inhomogeneous solutions that were unable to be electrospun.

2.3 Electrospinning of Aligned Fiber Mats

2.3.1 Sample Preparation

The same materials and methods described in Section 2.2.1 were used to prepare an electrospinning solution for aligned fiber mats. This time, however, only a 10wt% SP-PU solution was prepared since it proved to be most effective in the electrospinning of isotropic samples.

2.3.2 Electrospinning Parameters

Aligned fiber mats were created by electrospinning onto a MTI Corporation TC100 desktop spin coater, seen in **Figure 2.4**. The rotating metal disk of the spin coater was electrically grounded by bringing two heavy-gauged metal wires into physical contact with the side of the disk. These wires remained in contact with the disk during rotation and electrospinning. The wires were grounded via connection to the grounding screw of the fume hood. A rectangular piece of silicon wafer (n-type, phosphorus) was attached to the surface of the metal disk with carbon tape (**Figure 2.5)**. This created a raised conductive surface that could be removed to allow easier collection and inspection of the fiber mat samples. To determine the effect of rotation speed on nanofiber alignment, three different rotation speeds were used for the spin coater during electrospinning: 500, 2000, and 3000 rpm. The flow rate for the SP-PU

solution was held constant at 9 μL/min and the needle tip was separated by 10 cm from the surface of the metal disk. The applied voltage for each run was 11-12 kV. Each run was allowed to continue for 5-10 minutes, or until a visible layer of nanofibers had collected.

Figure 2.4. TC100 Spin Coater. *Note: The post, syringe holder, and plastic cover shown above were removed and the syringe+syringe pump was suspended above the metal disk.*

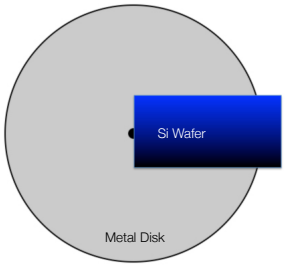

Figure 2.5. Illustration showing silicon wafer on metal disk of spin coater.

2.3.3 Fiber Alignment as a Function of RPM

A Hitachi S-4700 high-resolution scanning electron microscope (SEM) was used to inspect fiber alignment on the wafers at the three rotation speeds. To compare the alignment across the three speeds, the same relative location (about ¾ of the way along the wafer, moving

outwardly in a radial direction) of each wafer was chosen. The importance of this aspect is explained in a later section. At 500 rpm, the disk rotation was apparently too slow to orient the fibers in any discernible direction as they were deposited (**Figure 2.6**). At 2000 rpm, there was a significant degree of alignment imparted to the nanofibers, which can be seen in **Figure 2.7**. At 3000 rpm, there was also a degree of alignment among the nanofibers, but there was evidence of many broken fiber pieces. This indicated that the speed was too high and many fibers were ripped into pieces as they were deposited (**Figure 2.8**).

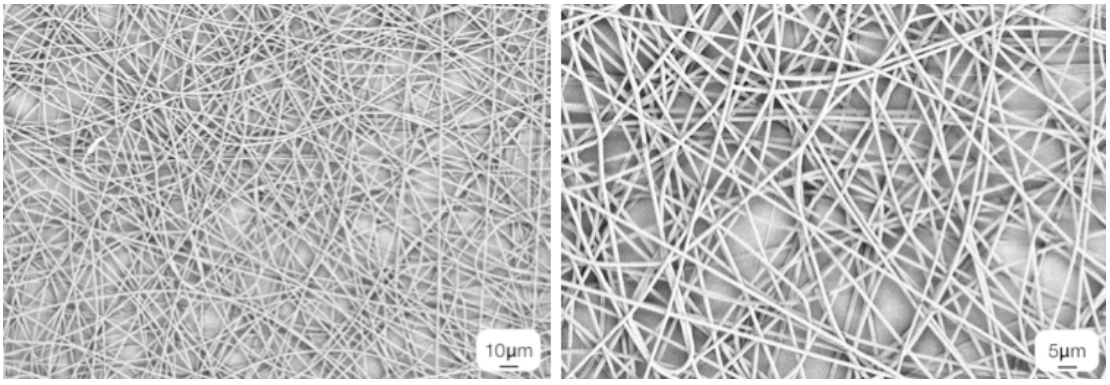

Figure 2.6. Fibers collected at disk speed of 500 rpm.

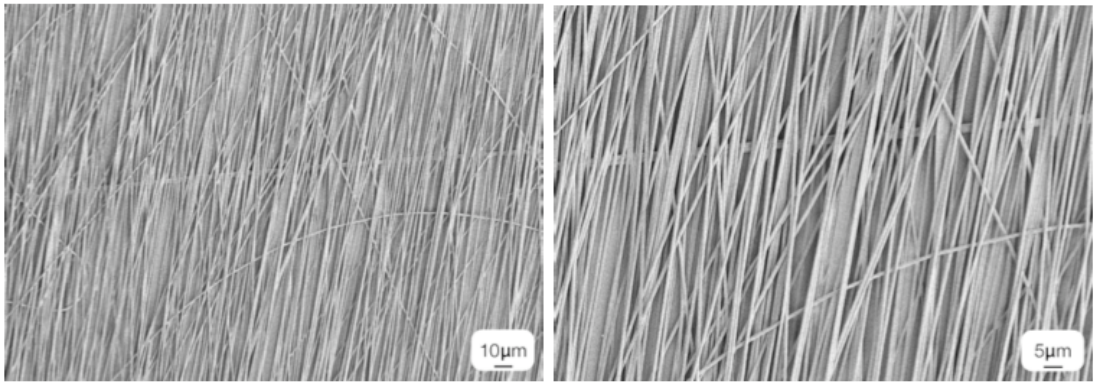

Figure 2.7. Fibers collected at disk speed of 2000 rpm.

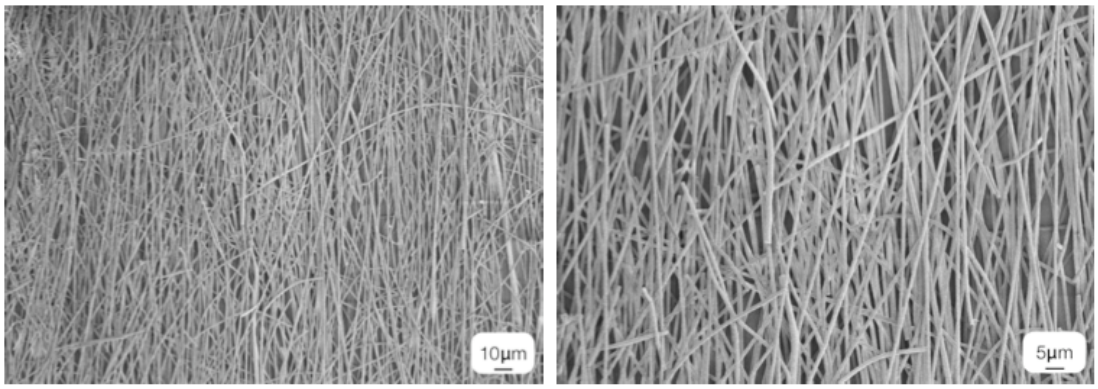

Figure 2.8. Fibers collected at disk speed of 3000 rpm.

2.3.4 Fiber Alignment as a Function of Surface Velocity

In addition to having various degrees of alignment at different rotation speeds, the position along the wafer at a given rpm was also important. The surface velocity of the metal disk/silicon wafer is not constant; it increases as you move radially from the center of the metal disk. For instance, the orientation of the nanofibers changed from completely random to significantly aligned along the wafer at 2000 rpm (**Figure 2.9**). Therefore, the location of maximum alignment, or "sweet spot," was the only part of the fiber mat collected for mechanical tests.

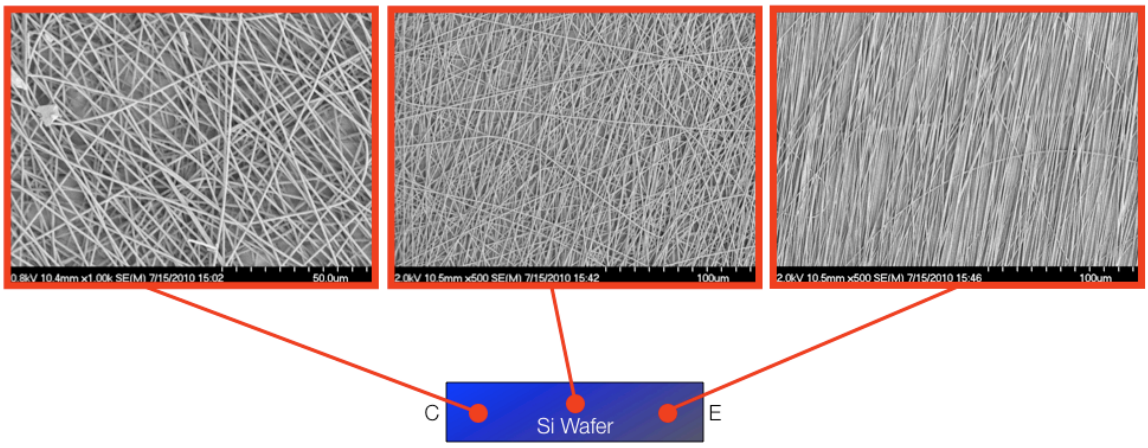

Figure 2.9. Variation of fiber alignment based on position along silicon wafer. "C" denotes the part of the wafer located at the center of the disk while "E" represents the edge, or the section farthest out radially.

2.3.5 Two-Dimensional Fast Fourier Transform Analysis

Quantification of nanofiber alignment was accomplished using a two-dimensional fast Fourier transform (2D FFT) approach with the aid of ImageJ software[9] supported by an oval profile plug-in (authored by William O'Connnell). A detailed account of the theory and application of 2D FFT has been described previously by Ayres *et al.*[10] Briefly, a micrograph of an electrospun mat is composed of pixels that depict the spatial organization of its constituent fibers. The 2D FFT function transforms this spatial data into a mathematically defined frequency domain that maps the change of pixel intensities across the original data image.

The 2D FFT analysis was performed on three different sections of a single wafer used to collect fibers at 2000 rpm (**Figure 2.10**). 0° was arbitrarily set at the 12 o'clock position of the micrograph and the azimuthal angle increases clockwise around the image. A peak in the FFT intensity (ordinate) at a given angle indicates the direction in which the fibers are oriented, and since each fiber intersects the micrograph border at two locations, it is responsible for contributing to the intensity at two different angles. Therefore, a large intensity at two azimuthal angles denotes significant fiber alignment in that particular direction. For the randomly aligned

sample (Figure 2.10a), no large peaks in intensity can be seen. For the partially aligned and aligned samples (Figures 2.10b and 2.10c, respectively), two peaks at 10° and 190° are observable. As expected the peaks are much more intense and the baseline is reduced in the 2D FFT analysis of the aligned sample.

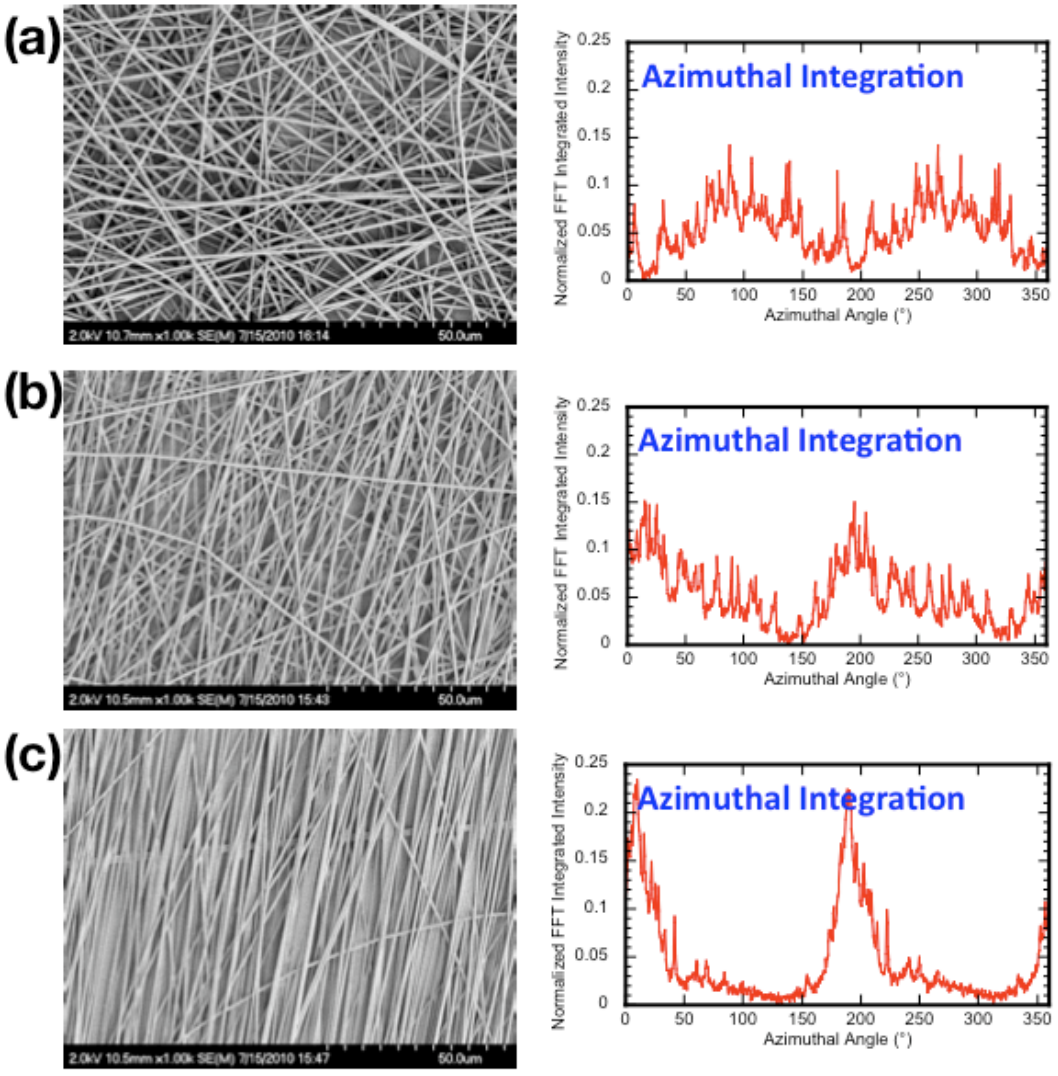

Figure 2.10. Micrographs of (a) random, (b) partially aligned, and (c) aligned sections of fiber mat and the corresponding 2D FFT analyses.

2.3.6 Mechanical Testing of Aligned Fiber Bundles

2.3.6.1 Collection of Aligned Fiber Mats and Experimental Setup

The same silicon wafer-spin coater setup was used to prepare samples for mechanical testing. The only adjustment of procedure was that each electrospinning run was allowed to continue at 2000 rpm for 20-30 minutes, which allowed for the formation of mats robust enough for mechanical testing. After electrospinning, the silicon wafer was removed from the metal disk and the fiber mat was rolled onto itself in the direction perpendicular to the length of the wafer (**Figure 2.11**). This resulted in fiber bundles with nanofiber alignment in the longitudinal direction of the bundle (**Figure 2.12**).

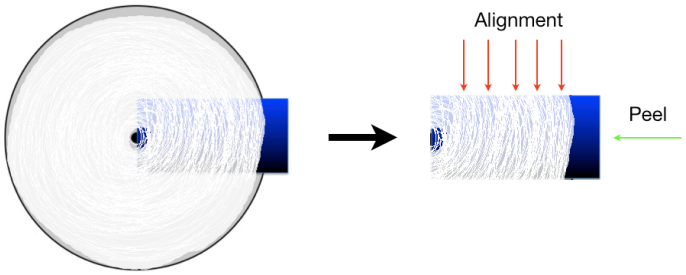

Figure 2.11. Illustration depicting collection of aligned fiber mats.

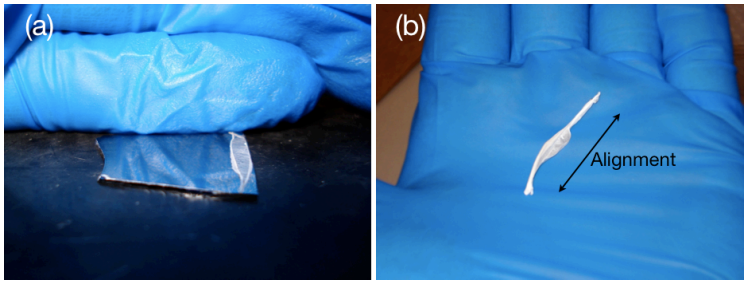

Figure 2.12. (a) Partially rolled fiber bundle on silicon wafer and (b) fiber bundle with nanofiber alignment in longitudinal direction.

Mechanical tests of the sample were accomplished using a custom-designed micro-load frame. The two ends of each bundle were held using blocks and tension screws (**Figure 2.13**). Initially, a micro-load cell was used to record stress-strain data over the course of the mechanical tests. However, the load cell had a maximum load capacity of several grams, and this was not enough to cause significant stretching of the fiber bundle. Therefore, the load cell was removed and only the load frame was used.

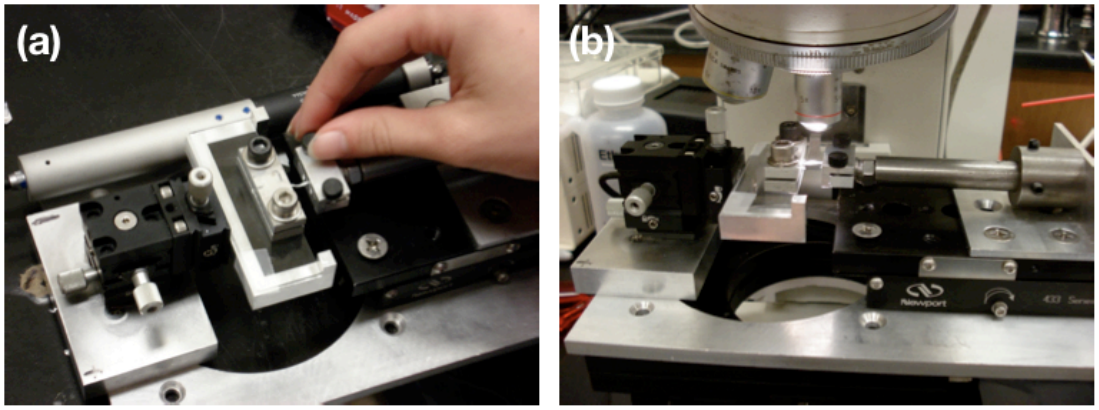

Figure 2.13. (a) Fiber bundle in load cell and (b) load cell on microscope stage.

Due to the fact that only a small amount of material, and thus mechanophore, was present in the fiber bundles, fluorescence detection was used to observe if mechanical activation of spiropyran occurred. As stated previously, the merocyanine (activated) form of the mechanophore is fluorescent while the spiropyran (non-activated) form is not. The mechanical tests were performed under observation in a fluorescent microscope with excitation from a 100-Watt mercury arc lamp at 525 nm.

2.3.6.2 Control Experiment and Free Fiber Bundles

Initial mechanical tests were performed on what will be referred to as "free" fiber bundles. These are fiber bundles, shown in Figure 2.12b, that are only bound together by inter-nanofiber forces.

To ensure the spiropyran-merocyanine transition within the fiber bundles can be observed in the fluorescence microscope, the fiber bundles were exposed to long wave ultraviolet light (365 nm). As stated previously, the activation of this particular mechanophore can be accomplished in a number of ways, including by exposure to ultraviolet light. **Figure 2.14** shows the fiber bundle, as observed under the fluorescent microscope, both before and after UV exposure. There is a clear increase in fluorescence in the post-exposure image, which indicates that mechanical activation of the mechanophores in the fiber bundle should be easily observable.

Each bundle was deformed at a strain rate of 0.040 mm/sec. No obvious increase in fluorescence from the bundles was detected at strains as high as 600% (**Figure 2.15**). The spiropyran-polyurethane dog bones mentioned previously experience significant mechanophore activation at strains greater than 100%. Therefore, some other mechanism must have occurred to allow very little stress to be imparted to the spiropyran-polyurethane nanofibers. Although robust, the bundles were a loose collection of nanofibers. It is possible these fibers were simply slipping past one another within the bundle without having any force transmitted to them. This would explain the ability of the bundle to experience significant strains while simultaneously showing no mechanical activation of the mechanophores.

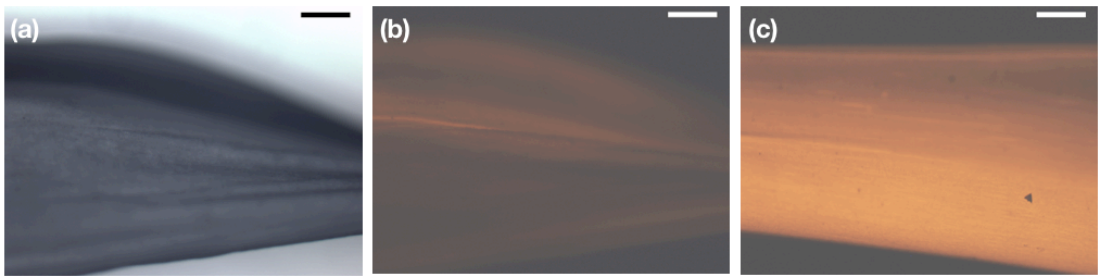

Figure 2.14. (a) Optical image of fiber bundle. (b) Fluorescence image of fiber bundle before and (c) after UV exposure (scale bars = 5 mm). *Note: Images (a), (b) are from same part of fiber bundle. Image (c) is of a different section since the fiber bundle had to be removed from microscope for UV exposure.*

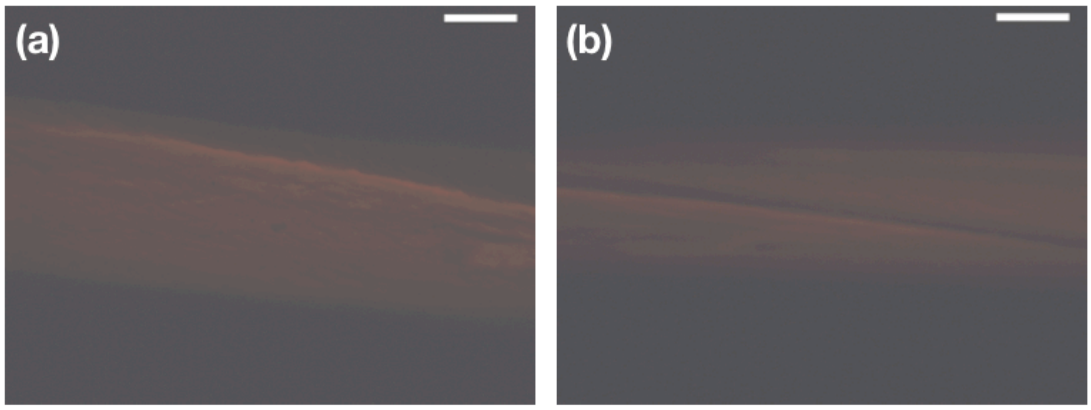

Figure 2.15. Fluorescence images of fiber bundle (a) before mechanical deformation and (b) after 600% strain. The lack of change in fluorescence intensity indicates no mechanophore activation (scale bars = 5 mm).

2.3.6.3 Glued Fiber Bundles

To minimize nanofibers slipping past one another within the bundle, the ends of each bundle were glued to a substrate. The glue droplets were placed as close as possible to each other along the bundle in an attempt to "grab" both ends of as many nanofibers as possible. However, the glue droplets needed to be separated by enough distance that they did not wet along the fiber and combine.

The fiber bundles were laid across a hole cut into a small piece of aluminum foil. The size of the hole, and therefore the gauge length of the fiber bundles, was varied to determine the effect, if any, on activation. A small drop of Loctite® 495 Instant Adhesive was placed at the

end of each bundle. Only a small amount of glue was used in an attempt to ensure that the glue did not travel across the gauge length of the bundle (**Figure 2.16**). The glue was allowed to dry overnight and the bundles were mechanically tested in the same fashion as the free fiber bundles. Although it was not obvious when inspecting the fiber bundles, the glue had apparently wicked across the gauge length and embrittled the bundles. As a result, the nanofiber-superglue bundles failed almost immediately during mechanical tests and no activation of the mechanophores was observed.

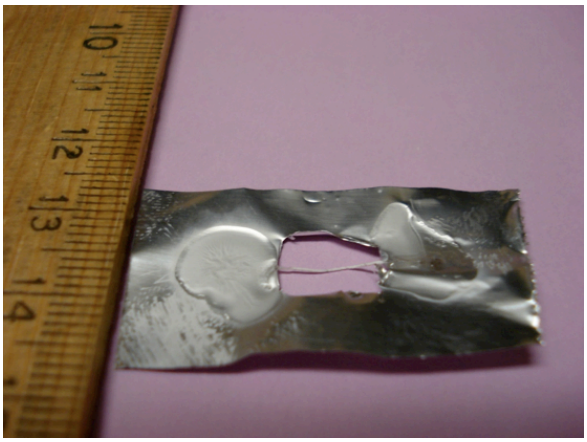

Figure 2.16. Fiber bundle glued to aluminum foil testing frame. *Note: The sides of the frame were severed prior to mechanical testing.*

2.4 Summary

Spiropyran-polyurethane nanofibers were prepared by electrospinning and these nanofibers were collected into aligned macroscopic bundles amenable to mechanical testing. Although the free bundles proved to be quite robust during deformation, no mechanical activation of the spiropyran was detected even at very large strains. In an attempt to secure the nanofibers within the mat, the bundles were subsequently glued at each end prior to mechanical

testing. However, this resulted in brittle nanofiber-superglue bundles that failed before any mechanophore activation was observed.

2.5 References

1. Beiermann, B. A.; Kramer, S. L. B.; Moore, J. S.; White, S. R.; Sottos, N. R., *ACS Macro Letters* **2012,** *1* (1), 163-166.

2. Demir, M. M.; Yilgor, I.; Yilgor, E.; Erman, B., *Polymer* **2002,** *43* (11), 3303-3309.

3. Theron, S. A.; Zussman, E.; Yarin, A. L., *Polymer* **2004,** *45* (6), 2017-2030.

4. Khil, M. S.; Cha, D. I.; Kim, H. Y.; Kim, I. S.; Bhattarai, N., *J. Biomed. Mater. Res. Part B* **2003,** *67B* (2), 675-679.

5. Stankus, J. J.; Guan, J. J.; Fujimoto, K.; Wagner, W. R., *Biomaterials* **2006,** *27* (5), 735-744.

6. Guelcher, S. A., *Tissue Eng. Part B-Rev.* **2008,** *14* (1), 3-17.

7. Pedicini, A.; Farris, R. J., *Polymer* **2003,** *44* (22), 6857-6862.

8. Lee, C. K.; Davis, D. A.; White, S. R.; Moore, J. S.; Sottos, N. R.; Braun, P. V., *Journal of the American Chemical Society 132* (45), 16107-16111.

9. Rasband, W. S. *ImageJ*, U.S. National Institutes of Health: Bethesda, Maryland, USA, 1997-2012.

10. Ayres, C. E.; Jha, B. S.; Meredith, H.; Bowman, J. R.; Bowlin, G. L.; Henderson, S. C.; Simpson, D. G., *J Biomater Sci Polym Ed* **2008,** *19* (5), 603-21.

CHAPTER THREE

ELECTROSPINNING OF *gem*-DIBROMOCYCLOPROPANE MECHANOPHORES

3.1 Introduction and Motivation

In addition to being used to produce new classes of materials from existing mechanophore-polymer systems, electrospinning also has the potential for use in the area of novel mechanophore development. The primary method of testing new mechanophores early in their development cycle has been sonication.[1-5] The physical effects of sonication have been investigated for a number of systems including polymer membranes,[6] proteins,[7] carbon nanotubes,[8] and polymer chains.[9, 10]

The mechanochemical effect of sonication arises from the phenomenon known as cavitation, which involves the formation, growth, and collapse of bubbles (**Figure 3.1**). These bubbles are generated by the pressure gradient formed in a solution during intense ultrasonic radiation. The bubble collapse is a very rapid and violent event, and this pulls nearby polymer molecules toward the cavity of the bubble.[11] As one end of the polymer chain is pulled, solvodynamic shear creates a mechanical stress along the backbone of the polymer. If the molecule is large enough, chain scission is possible and usually occurs near the midpoint of a homopolymer, where shear forces are typically strongest.[12] However, preferential mechanochemical events can occur prior to chain scission if a weakened bond, like that in a mechanophore, is incorporated into the polymer.[13]

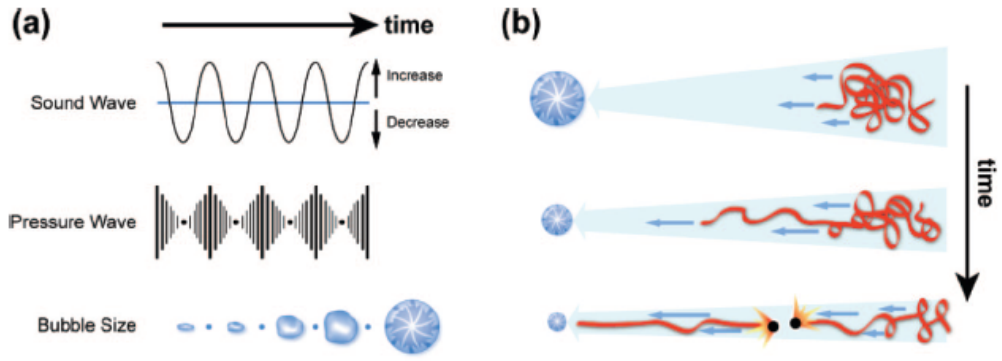

Figure 3.1. Mechanism of mechanochemical effects via ultrasound. (a) Variations in pressure result in the gradual formation of bubbles in the solution. (b) Polymer backbone experiences significant stresses (enough to cause bond scission in this depiction) as one end is drawn toward the rapidly collapsing bubble. Adapted from Caruso *et al.*[12]

Although sonication has proven effective in prior mechanochemistry studies, it is not without its disadvantages. For one, bubble formation is a highly specific process and can be affected by a number of different factors including choice of solvent,[14] temperature,[15] ultrasound intensity,[16] and concentration.[17] Vapor pressure is the most influential solvent property in regards to cavitation, and thus mehcanochemical events, and it was investigated by Madras *et al.*[18] It was discovered that increases in solvent vapor pressure had adverse affects on chain scission rates. Higher temperatures have also been found to adversely affect the occurrence of chain scission during sonication.[19, 20] In addition, sonication can cause the transformation of solvent or other small molecules into radical species (**Figure 3.2**). The reactive byproducts can result in undesirable side reactions with the polymer of interest, which could interfere with the current mechanochemistry investigation.[21] Furthermore, sonication requires relatively low concentrations of polymer in solution and the mechanical effects take place over very short distances (on the order of micrometers).[11] This results in an inexact time frame for the course of the experiment and sonications are commonly performed for long periods of time to ensure the mechanochemical reactions have occurred.

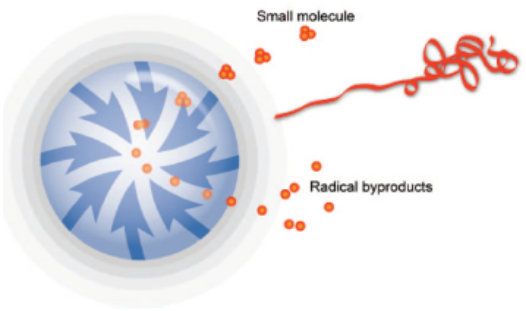

Figure 3.2. Formation of radical byproducts during bubble collapse. Adapted from Caruso *et al.*[12]

In contrast, electrospinning is a much more straightforward and controllable process. It is amenable to a multitude of solvents and, although an adjustment to experimental parameters may be necessary, the only requirement is that the particular polymer has moderately high solubility in the given solvent.[22, 23] Also, electrospinning is easily performed at room temperature and produces none of the undesirable reactive species like sonication. And finally, the electrospinning process yields solid polymeric nanofibers that can then be directly transferred to characterization-specific solvents (deuterated solvents for NMR, high-purity chromatographic solvents, etc.).

Electrospinning has been previously utilized to mechanically deform bio-polymers in solution.[24, 25] By electrospinning double-stranded DNA (ds-DNA) with polyethylene oxide nanofibers, Bellan and coworkers were able to trap significantly elongated DNA molecules and fragments of DNA molecules.[24] This elongation and fragmentation of ds-DNA suggests the forces during electrospinning were strong enough to stretch and, in some cases, break the DNA backbone.

There has been some work to quantify the mechanical forces on polymer chains during electrospinning.[26, 27] Han *et al.* exclusively examined the transition zone of an electrospinning

jet (**Figure 3.3**) and measured longitudinal stresses to be on the order of 100 kPa with stretching rates on the order of 100-1000 s^{-1}.[26] Strain rates, however, are much more intense during the whipping and bending part of the electrospinning jet (**Figure 3.4**), and the longitudinal strain rate in a whipping electrospinning jet was estimated to be on the order of 10^5 s^{-1} by Reneker and coworkers.[27] This is within an order of magnitude of the strain rates experienced during sonication, which are in the range of 10^5-10^6 s^{-1} (**Figure 3.5**).[12]

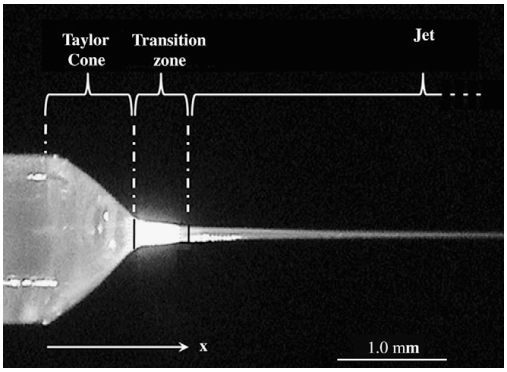

Figure 3.3. The three zones of an electrospinning jet. Adapted from Han *et al*.[26]

Figure 3.4. High-speed photograph of a whipping electrospinning jet. Adapted from Reneker *et al*.[27]

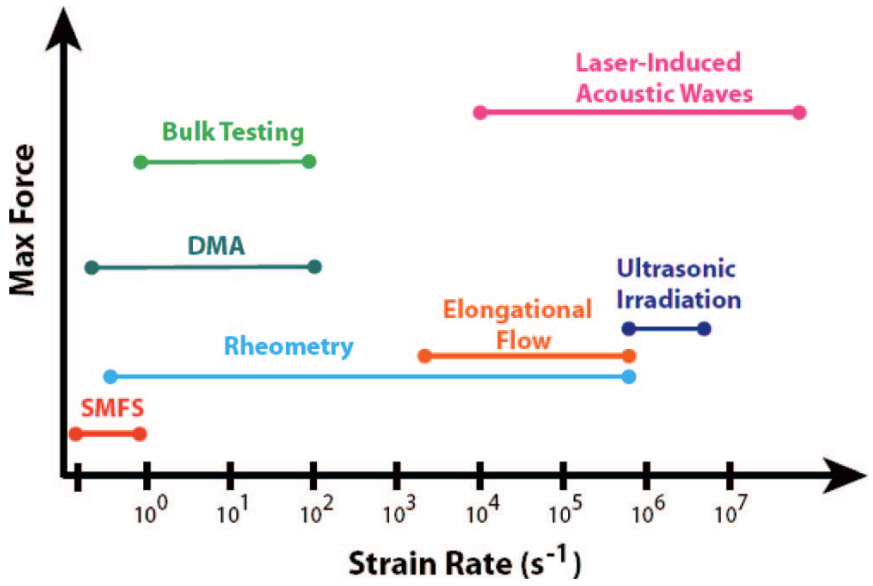

Figure 3.5. Summary of experimental methods for the determination of mechanochemical activity. Adapted from Caruso *et al.*[12]

This research investigates if the forces during electrospinning are enough to result in the activation of a mechanophore-functionalized polymer. A reversible mechanophore, such as spiropyran, would not be suitable for such an experiment as it could revert back to its inactivated form after being incorporated into nanofibers. Therefore, the previously mentioned *gem*-dibromocyclopropane (**Figure 1.8b**), an irreversible mechanophore, will be used.

3.2 Experimental

3.2.1 Sample Preparation

A 300 kDa *gem*-dibromocyclopropane (*g*DBC) polymer was prepared by Ashley L. Black of the Stephen L. Craig group at Duke University, and the synthetic procedure has been previously reported.[28] Initially, a 1:1 mixture of THF/DMF, since it performed well in previous experiments, was going to be used as the electrospinning solvent. However, the *g*DBC polymer had very low solubility in the mixture so neat THF was used. 0.3602 g polymer was dissolved in

4 mL THF to yield a 10-wt% solution. The solution was subjected to magnetic stirring and slight heating (40°C) for two hours to aid in the dissolution of the polymer. Special care had to be taken when exposing the polymer to heat as temperatures greater than 40°C or long-term (> 6 hours) exposure to room temperature would result in the auto-activation of the mechanophore. Therefore, the polymer was kept at 0°C when not in use. The polymer solution was transferred to a 10-mL syringe fitted with a 23-gauge hypodermic needle that had been previously ground flat using a bench grinder.

3.2.2 Electrospinning Parameters

The polymer solution was fed at a constant rate via a syringe pump (KDScientific) that was suspended 8 cm above a grounded copper wire mesh with a diameter of 10 cm. For electron microscopy samples, a small piece of silicon wafer (n-type, phosphorus) was placed on the copper wire grid. For NMR studies, a maximum collection area was desired so the wire mesh was covered with aluminum foil. The feed rate was fixed at 5 μL/min and the metallic needle was connected to a 30 kV high-voltage power supply (RHR30PN10, Spellman). The applied voltages for electrospinning ranged from 5-8 kV. Achieving a Taylor cone was very difficult for the polymer solution and the ones that were achieved were short-lived. As a result, both microscopy and NMR were performed on an extremely low concentration of fibers. It is believed this difficulty was a result of the high volatility of the electrospinning solvent (THF) and the poor solubility of the polymer, which might have resulted in undetectable solution inhomogeneities.

In parallel to the electrospinning experiments, a few milligrams of *g*DBC was removed from the freezer and dissolved in $CDCl_3$. This solution was kept at the same temperature (40°C

and room temperature) as the electrospinning solution at all times to rule out the possibility of thermal activation of the mechanophore.

3.3 Analysis of Electrospun *g*DBC Fibers

3.3.1 Scanning Electron Microscopy

A Hitachi-S4700 high-resolution scanning electron microscope (SEM) was used to inpspect the *g*DBC nanofiber formation on the wafer, preceded by sputtering with Au/Pd. Electrospinning the *g*DBC solution proved quite difficult so only a small amount of fibers were collected for microscopy (**Figure 3.6**). SEM was performed to confirm the desired fiber morphology was present since thin fibers suggest it was more likely the polymer chains endured fairly high strain rates during the whipping and thinning process described previously in this chapter. Although some beads are present on the fibers, they are in low enough concentration that a significant portion of the polymer should have been exposed to high strain rates, if they occurred.

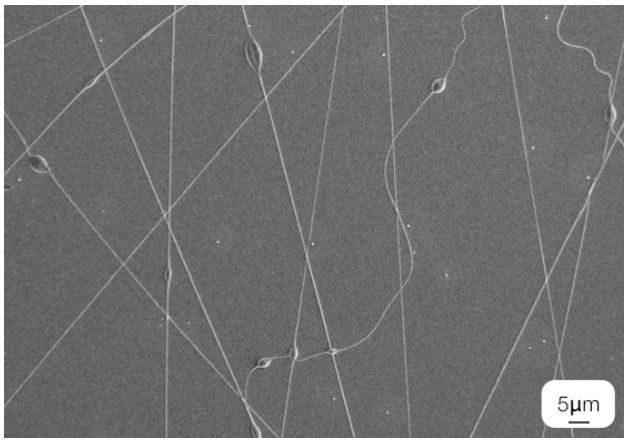

Figure 3.6. Micrograph of *g*DBC nanofibers on silicon wafer.

3.3.2 Nuclear Magnetic Resonance (NMR) Spectroscopy

After electrospinning, the small amount of nanofibers on the aluminum foil collector was placed in the freezer overnight to prevent activation and allow complete evaporation of the electrospinning solvent. The *g*DBC/$CDCl_3$ control sample was also placed in the freezer (capped) overnight. The area of interest on the aluminum foil was then rinsed with as little $CDCl_3$ as possible, and this rinse was transferred via pipette to a NMR tube. The control sample was also transferred to a separate NMR tube. ^{1}H-NMR spectroscopy, courtesy Brian Steinberg and Ariane Vartanian, was performed using a Varian VXR 500 MHz spectrometer.

As stated in the introductory chapter, the *g*DBC mechanophore activation is determined by NMR spectroscopy. Specifically, mechanical activation of the mechanophore-polymer results in the formation and increase of two characteristic peaks at 6.1 and 4.6 ppm (**Figure 3.7**). In the case of Figure 3.7, the mechanical forces during the extrusion process were used to activate the mechanophore. However, prior sonication experiments were also used to cause activation and the formation of the same ^{1}H-NMR peaks was observed. The ^{1}H-NMR spectrum for the control (non-electrospun) *g*DBC polymer sample is shown in **Figure 3.8**. As expected, there are no peaks at 6.1 or 4.6 ppm, indicating the mechanophore had not been activated.

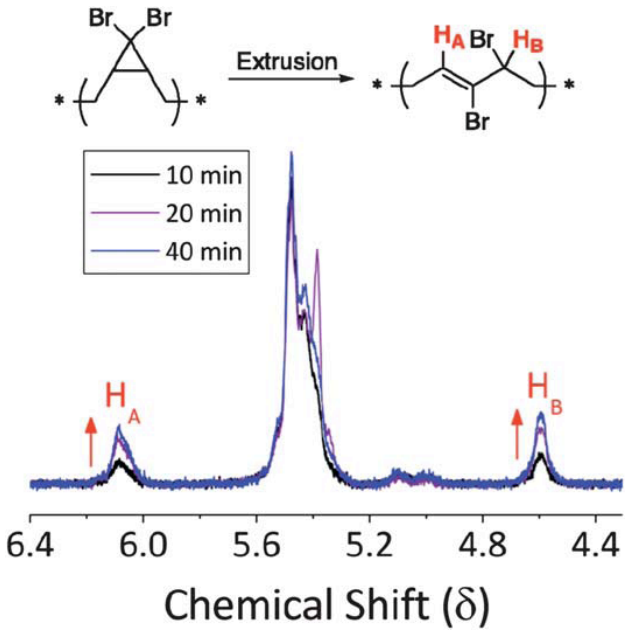

Figure 3.7. Growth of proton peaks H_A and H_B corresponding to mechanophore activation during extrusion of mechanphore-polymer. Longer extrusion times resulted in increased peak intensities (more mechanophore activation). Adapted from Black *et al.*[28]

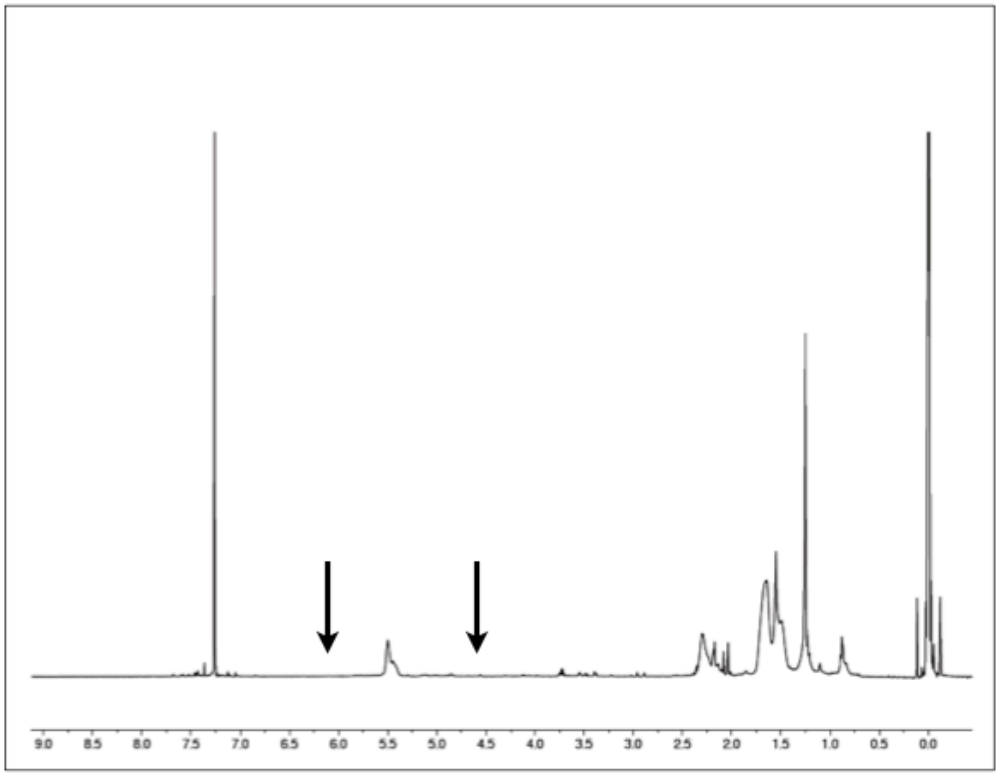

Figure 3.8. ^{1}H-NMR spectrum for *g*DBC control sample. Black arrows indicate absence of characteristic peaks, suggesting mechanophore had not activated.

The ^{1}H-NMR spectrum for the electrospun sample is show in **Figure 3.9**. The very small amount of electrospun fibers collected required that the spectrum be amplified. This results in a noisier baseline and causes some peaks to appear more exaggerated than they would be in a more concentrated sample. As with the control, there are no characteristic peaks evident at 6.1 or 4.6 ppm, indicating that the forces present during electrospinning were not enough to activate the mechanophore. The electrospun sample is not exactly the same as the control, however, as it appears the methods used for electrospinning may have introduced impurities into the sample. In addition to the increase in size caused by amplification, there is an extra peak in the group ranging from 4.0 to 3.4 ppm (blue bracket in Figure 3.9). Although the exact cause for this peak is still unknown, this can most likely be attributed to an impurity that was introduced during the electrospinning process. This impurity could have been introduced during a number of steps, but most likely is a result of the exposure to a contaminant on the aluminum foil, electrospinning solvent, or air. Another difference in the electrospun sample spectrum is the increase in the water peak at ~1.5 ppm. This water uptake most likely occurred when the nanofibers were allowed to sit uncovered in the freezer overnight.

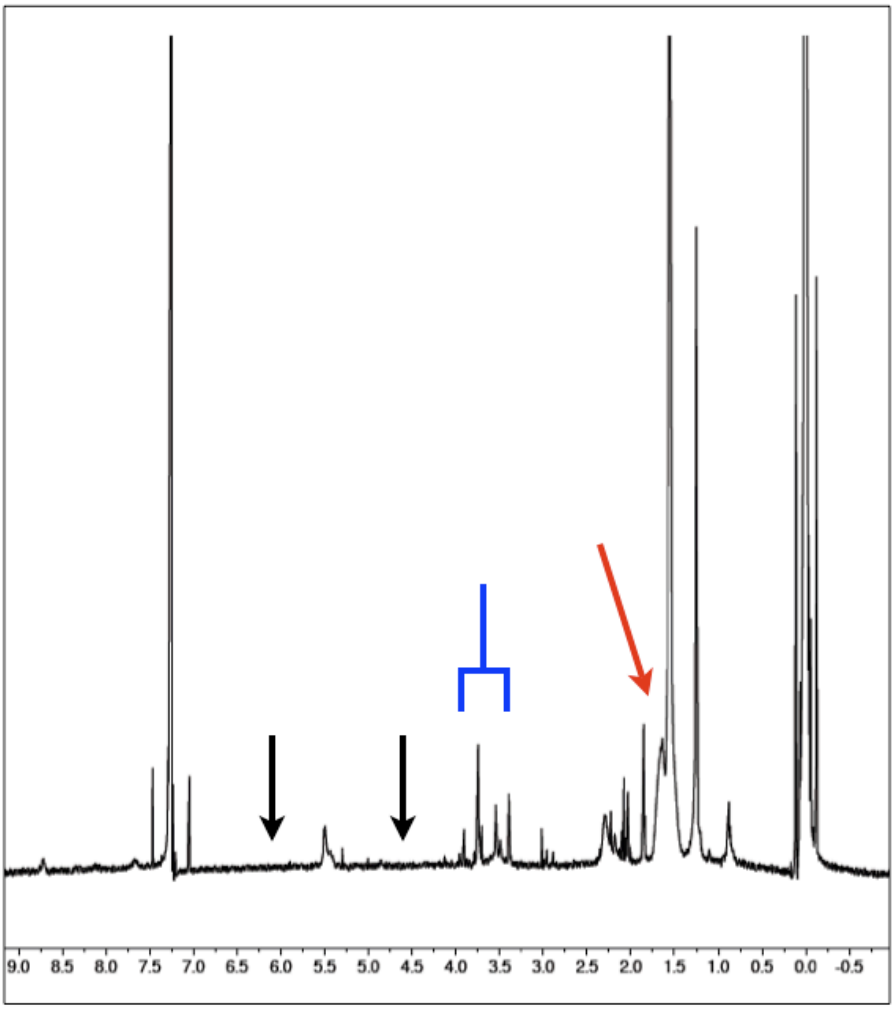

Figure 3.9. ^{1}H-NMR spectrum for *g*DBC electrospun sample. Note the lack of activation peaks (black arrows), additional peak within 4.0 to 3.4 ppm (blue bracket), and increased water peak (red arrow).

3.4 Additional Experiments

The electrospinning of *g*DBC was repeated multiple times using tetrahydrofuran. The electrospinning parameters were manipulated during these experiments in order to attain the highest longitudinal strain possible. This included increasing the needle-collector distance and voltage to the maximum safe allowances. At these conditions, however, electrospinning did not occur and nanofibers were not able to be collected. Electrospinning with chloroform, the only other solvent *g*DBC is moderately soluble in, was also tried, but attempts did not prove successful.

3.5 Summary

Nanofibers containing the irreversible *gem*-dibromocyclopropane mechanophore were successfully prepared via electrospinning. The nanofibers were analyzed by NMR spectroscopy to determine if the longitudinal forces and strain rates during electrospinning were significant enough to cause activation of the mechanophore. No mechanophore activation was detected, indicating the current experimental setup is not sufficient to achieve adequate longitudinal stresses.

3.6 References

1. Hickenboth, C. R.; Moore, J. S.; White, S. R.; Sottos, N. R.; Baudry, J.; Wilson, S. R., *Nature* **2007,** *446* (7134), 423-7.

2. Kryger, M. J.; Ong, M. T.; Odom, S. A.; Sottos, N. R.; White, S. R.; Martinez, T. J.; Moore, J. S., *J. Am. Chem. Soc. 132* (13), 4558-4559.

3. Potisek, S. L.; Davis, D. A.; Sottos, N. R.; White, S. R.; Moore, J. S., *J. Am. Chem. Soc.* **2007,** *129* (45), 13808-13809.

4. Wiggins, K. M.; Hudnall, T. W.; Shen, Q.; Kryger, M. J.; Moore, J. S.; Bielawski, C. W., *J. Am. Chem. Soc. 132* (10), 3256-3257.

5. Lenhardt, J. M.; Black, A. L.; Craig, S. L., *Journal of the American Chemical Society* **2009,** *131* (31), 10818-10819.

6. Masselin, I.; Chasseray, X.; Durand-Bourlier, L.; Lainé, J.-M.; Syzaret, P.-Y.; Lemordant, D., *Journal of Membrane Science* **2001,** *181* (2), 213-220.

7. Bradbury, J. H.; O'Shea, J., *Aust. J. Biol. Sci.* **1973,** *26* (3), 583-590.

8. Hennrich, F.; Krupke, R.; Arnold, K.; Rojas Stütz, J. A.; Lebedkin, S.; Koch, T.; Schimmel, T.; Kappes, M. M., *The Journal of Physical Chemistry B* **2007,** *111* (8), 1932-1937.

9. Grönroos, A.; Pirkonen, P.; Heikkinen, J.; Ihalainen, J.; Mursunen, H.; Sekki, H., *Ultrasonics Sonochemistry* **2001,** *8* (3), 259-264.

10. Suslick, K. S.; Price, G. J., *Annu. Rev. Mater. Sci.* **1999,** *29*, 295-326.

11. Paulusse, J. M. J.; Sijbesma, R. P., *Journal of Polymer Science Part A: Polymer Chemistry* **2006,** *44* (19), 5445-5453.

12. Caruso, M. M.; Davis, D. A.; Shen, Q.; Odom, S. A.; Sottos, N. R.; White, S. R.; Moore, J. S., *Chemical Reviews* **2009,** *109* (11), 5755-5798.

13. Encina, M. V.; Lissi, E.; Sarasúa, M.; Gargallo, L.; Radic, D., *Journal of Polymer Science: Polymer Letters Edition* **1980,** *18* (12), 757-760.

14. Koda, S.; Mori, H.; Matsumoto, K.; Nomura, H., *Polymer* **1994,** *35* (1), 30-33.

15. Casale, A., *Journal of Applied Polymer Science* **1975,** *19* (5), 1461-1473.

16. Price, G. J.; Smith, P. F., *Polymer* **1993,** *34* (19), 4111-4117.

17. Jellinek, H. H. G.; White, G., *Journal of Polymer Science* **1951,** *7* (1), 33-37.

18. Madras, G.; Chattopadhyay, S., *Polymer Degradation and Stability* **2001,** *71* (2), 273-278.

19. Mauler, R. S.; Guaragna, F. M.; Gobbi, D. L.; Samios, D., *European Polymer Journal* **1997,** *33* (3), 399-402.

20. Chakraborty, J.; Sarkar, J.; Kumar, R.; Madras, G., *Polymer Degradation and Stability* **2004,** *85* (1), 555-558.

21. Price, G. J.; Garland, L.; Comina, J.; Davis, M.; Snell, D. J.; West, P. J., *Research on Chemical Intermediates* **2004,** *30* (7), 807-827.

22. Wannatong, L.; Sirivat, A.; Supaphol, P., *Polymer International* **2004,** *53* (11), 1851-1859.

23. Choktaweesap, N.; Arayanarakul, K.; Aht-ong, D.; Meechaisue, C.; Supaphol, P., *Polym. J* **2007,** *39* (6), 622-631.

24. Bellan, L. M.; Cross, J. D.; Strychalski, E. A.; Moran-Mirabal, J.; Craighead, H. G., *Nano Lett* **2006,** *6* (11), 2526-30.

25. Takahashi, T.; Taniguchi, M.; Kawai, T., *Jpn. J. Appl. Phys. Part 2 - Lett. Express Lett.* **2005,** *44* (24-27), L860-L862.

26. Han, T.; Yarin, A. L.; Reneker, D. H., *Polymer* **2008,** *49* (6), 1651-1658.

27. Reneker, D. H.; Yarin, A. L.; Fong, H.; Koombhongse, S., *J. Appl. Phys.* **2000,** *87* (9), 4531-4547.

28. Black, A. L.; Orlicki, J. A.; Craig, S. L., *Journal of Materials Chemistry* **2011,** *21* (23), 8460-8465.

CHAPTER FOUR

MULTI-FUNCTIONAL SPIROPYRAN-CONTAINING HYDROGELS

4.1 Introduction and Motivation

There has been considerable interest in the development of hydrogels with multiple functionalities. The addition of these functionalities to hydrogels gives one the ability to turn on or off the swelling of the hydrogel or, at the very least, alter its swelling profile. These functionalities include sensitivity to light, temperature, pH, specific analytes, and electric signal, or a combination of two or more of these sensitivities.[1] To the best of the author's knowledge, however, there has been very little investigation into the creation of mechanically-sensitive hydrogels.

A mechanically-sensitive hydrogel would require the inclusion of one or more types of mechanically-sensitive molecules, or mechanophores. A potentially useful mechanophore is the previously discussed spiropyran. In prior chapters, this molecule was of importance due to its ability to change colors or increase in fluorescence when mechanically perturbed. However, the mechanophore is also interesting because its activation causes a nonpolar-to-polar transition (**Figure 4.1**).

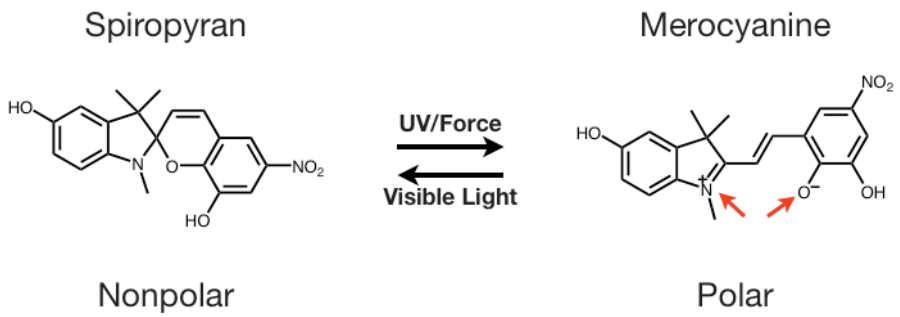

Figure 4.1. Transition of the spiropyran mechanophore from nonpolar form to polar merocyanine form.

The change in polarity, and hydrophilicity, has been used to alter the wetting properties of organic and inorganic surfaces. Samanta and Locklin[2] investigated the change in the contact angle of water droplets on a polymer brush functionalized with spiropyran molecules. Upon UV irradiation, which caused the transition to the merocyanine form, the contact angle for the water droplet decreased by as much as 15°, indicating the surface became more hydrophilic. Vlassiouk and coworkers[3] attached spiropyran to the surface of nanoporous alumina membranes and determined the change in wettability of the system upon exposure to UV irradiation. While in the spiropyran form, the membrane did not wet and did not allow the transport of water or ions. Once converted to the merocyanine form, however, the membrane became polar enough to allow water and ions to cross the membrane.

There has been much less work performed on the incorporation of spiropyran into polymer gels. Benito-Lopez *et al*.[4] were able to achieve photo-induced de-swelling of a spiropyran-containing ionic liquid polymer gel (**Figure 4.2**). After being polymerized *in situ* in microfluidic channels, the gels were rinsed with an acidic solution to "lock" the molecule in the merocyanine form. The polar gel remained swollen and thus functioned as a stop valve in the microfluidic channel. Upon visible illumination, however, the molecule transitioned to the nonpolar form and the gel would de-swell, allowing liquid to pass through the channel.

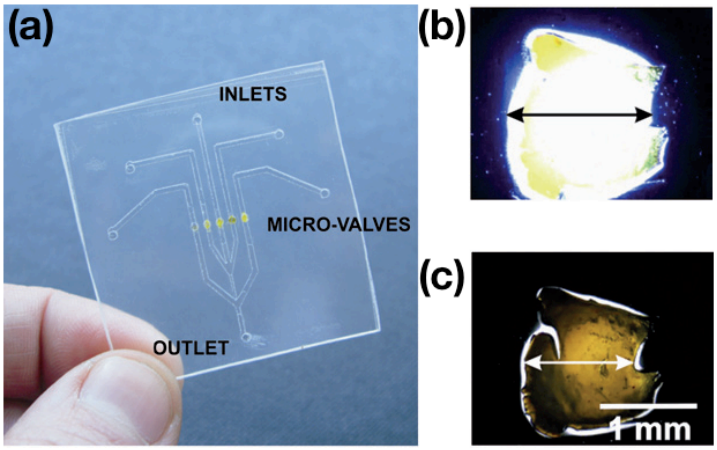

Figure 4.2. (a) Fabricated microfluidic device. (b) Merocyanine-ionogel under illumination with a white light LED [t = 0] and (c) spiropyran-ionogel after 2 s illumination, size decrease is *ca.* 30% by volume. Adapted from Benito-Lopez *et al.*[4]

Each of these three approaches has used light exposure, a relatively simple strategy to implement, to cause the spiropyran-merocyanine transition. When photo-switching is used, the molecule may be only anchored on one side and simply extend from the polymer backbone. Accordingly, a fairly large percentage of the spiropyran molecule can be incorporated into the polymer while having a minimal change on the overall mechanical properties. This high percentage (5% or greater) of spiropyran may be required to achieve the large-scale change in polarity within the hydrogel that is necessary to swell or de-swell the polymer.

Relying on mechanical force to achieve the same goal is significantly more complicated. In order to function as a mechanophore, the spiropyran must be anchored by polymer chains on both sides of the molecule in order to transmit force across it. This requires that the molecule be incorporated either directly in the polymer backbone or as a crosslinker between polymer chains. As such, only a relatively small percentage (1% or less) of mechanophore can be used without significantly changing the mechanical properties. Relying on such a small quantity of mechanophore to cause a drastic change in water absorption requires precise tuning of the hydrophilicity within the hydrogel.

This research investigated if the mechanically-induced polarity change of the spiropyran-merocyanine transition was enough to cause a significant increase in the swelling of a hydrogel. In order for the mechanophore to be mechanically-accessible, it was incorporated as a crosslinker between the hydrogel polymer chains. To ensure the polymer network remained flexible (i.e. able to swell and de-swell) a maximum of 1-wt% mechanophore crosslinker was used.

4.2 Spiropyran-HEMA Hydrogels

4.2.1 Materials

The dihydroxyspiropryan mechanophore was prepared by Preston May and the synthetic procedure has been described previously.[5] Tetrahydrofuran (THF) and *N*,*N*-dimethylformamide (DMF) were purchased from Fisher and 1,4-diazabicyclo[2.2.2]octane (DABCO) was purchased from Aldrich. 4-4'-methylene bis(phenyl isocyanate) (MDI) and 2,2'-azobis(2-methylpropionitrile) (AIBN) were obtained from Sigma Aldrich. 2-Hydroxyethyl methacrylate (HEMA) was purchased from Sigma Aldrich and run through a basic alumina plug prior to use to remove the inhibitor.

4.2.2 Methods

The dihydroxy-substituted variant is the most easily synthesized form of spiropyran and was chosen as the mechanophore. In order to incorporate it into the backbone of the hydrogel, it was first functionalized with isocyanates and these isocyanates reacted with the pendant hydroxy groups of the HEMA backbone (**Figure 4.3**). The strategy of using urethane linkages as crosslinkers for HEMA polymers was developed previously.[6, 7]

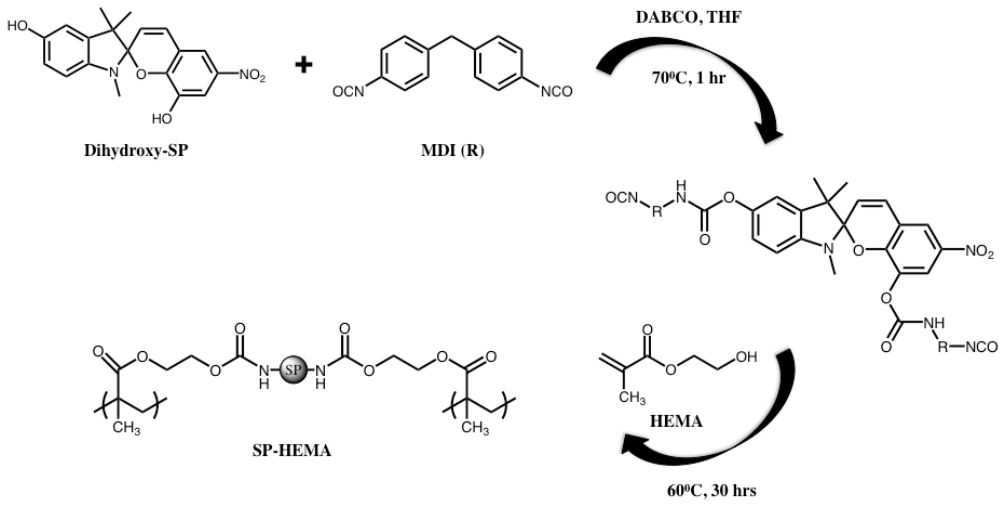

Figure 4.3. Isocyanate functionalization of dihydroxyspiropyran and crosslinking with HEMA pendant groups.

Dihydroxyspiropyran (36 mg, 0.102 mmol) was dissolved in 4 mL anhydrous THF in a 20-mL scintillation vial with a magnetic stirbar. DABCO (18.4 mg, 0.164 mmol) was added to the solution and the vial was purged with nitrogen for 5 minutes. MDI (48.0 mg, 0.192 mmol) was then added to the solution, and the vial was purged with nitrogen for an additional 5 minutes before being sealed and heated at 60°C for 1 hour (later extended to 2 hours). In a separate nitrogen-purged vial, AIBN (3.9 mg, 0.024 mmol) was dissolved in HEMA (6 mL, 49.5 mmol). The spiropyran-isocyanate solution was then mixed with the AIBN/HEMA solution and purged with nitrogen for 5 minutes. The vial was sealed and placed in a nitrogen-purged oven at 60°C for 30 hours.

4.2.3 Results

To recover the solid, dark purple polymer from the vial, the glass was broken with a hammer and the glass fragments were removed (**Figure 4.4**). To ensure proper crosslinking and remove any unreacted monomers, the polymer was allowed to soak in 20 mL DMF, a good

solvent for HEMA,[8] for 24 hours. However, after 24 hours the DMF solution was a very dark purple color and the hydrogel was significantly less colored (Figure 4.4b and c). The lack of color and poor mechanical integrity of the post-DMF gel indicated that the mechanophore was poorly functionalized and, thus, did not attach to the pendant groups of the HEMA backbone. Therefore, the initial reaction with the isocyanate (first step in Figure 4.3) was extended to 2 hours to allow for as much functionalization as possible. Reaction for longer time periods was also attempted, but the solution turned a slight pink color and this pink solution would not yield significantly crosslinked HEMA gels. It is likely the formation of the pink solution indicated further isocyanate reactions occurred and inert products were the result. The spiropyran-isocyanate mixtures that underwent 2-hour functionalization times were crosslinked into the HEMA gels at a much higher efficiency and did not leach out of the gel during DMF-induced swelling (**Figure 4.5**).

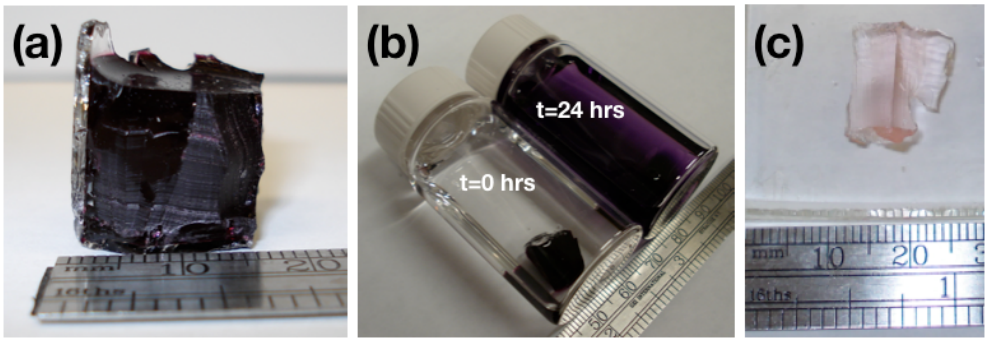

Figure 4.4. (a) SP-HEMA gel after polymerization. (b) SP-HEMA hydrogels in DMF at t=0 and t=24 hours. After 24 hours, significant SP was leached out into DMF solution. (c) SP-HEMA hydrogel after soaking in DMF for 24 hours. Very little color indicates only a small amount of SP was chemically bound into gel.

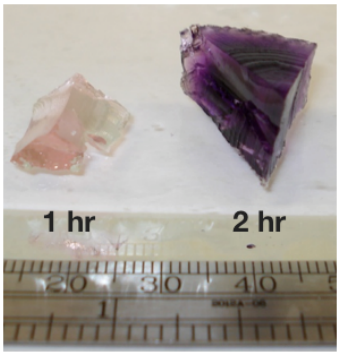

Figure 4.5. Comparison of 1- and 2-hour isocyanate functionalizations. The gel on the right retained more color, and thus crosslinker, when the 2-hour functionalization time period was used.

After the polymer was dry, it remained a dark purple color, indicating the mechanophore was in the polar merocyanine form. Therefore, the mechanophore needed to be reverted back to the nonpolar form so mechanical activation could cause swelling of the hydrogel. To achieve this, a small, thin piece of SP-HEMA gel was exposed to high intensity visible light under the microscope. Within five minutes, the entire sample was a slight yellow color, indicating the mechanophore was in the nonpolar spiropyran form. Approximately 60 seconds after the light source was removed, however, the entirety of the sample had returned to its original dark purple color (**Figure 4.6**). This experiment was repeated on several different slices of the SP-HEMA gel, both in hydrated and dehydrated states, but the same phenomenon was observed. This suggests the environment within the HEMA hydrogel is polar enough that the merocyanine form of the mechanophore is preferred. Therefore, the experiments with the HEMA-based hydrogels were abandoned and the search for a less polar polymer commenced.

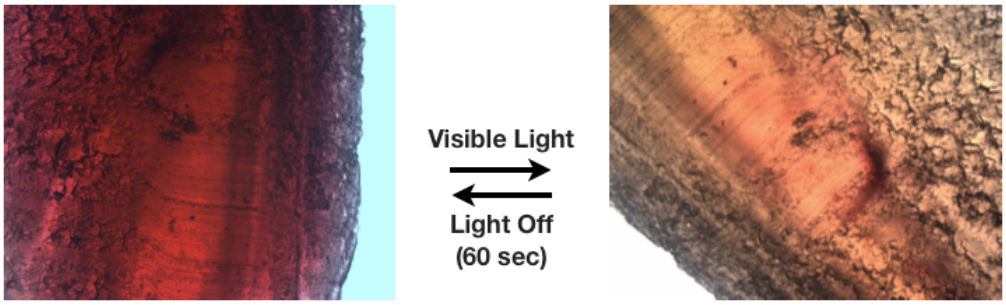

Figure 4.6. Photo-switching of mechanophore in SP-HEMA polymer. After removal of light source, mechanophore reverts back to polar merocyanine form.

4.3 Spiropyran-NIPAM Hydrogels

N-isopropylacrylamide (NIPAM) is a commonly used hydrogel polymer due to its ability to de-swell at increased temperatures. However, it is also interesting because it is slightly less polar than HEMA due to the presence of a hydrophobic isopropyl group extending from the nitrogen atom (**Figure 4.7**). There are also no pendant hydroxy-groups on the NIPAM monomer, so a mechanophore crosslinker with different functional groups was used.

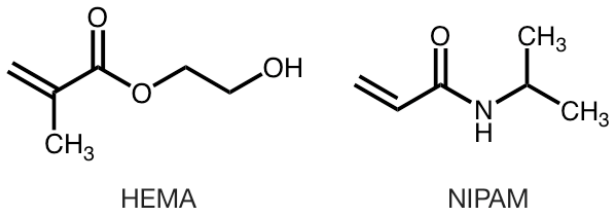

Figure 4.7. Molecular structures for HEMA and NIPAM monomers.

4.3.1 Materials

Diacrylate-spiropyran was prepared by Preston May and the synthetic procedure has been previously reported (**Figure 4.8**).[9] NIPAM monomer was purchased from Sigma Alridch and was purified by recrystallization from hexane. Briefly, 5 g NIPAM was dissolved in 60 mL hexane at 40°C. The solution was allowed to cool to room temperature, causing the NIPAM to

precipitate, and the solid was filtered and let air-dry. AIBN was also purchased from Sigma Alrich and used without further purification.

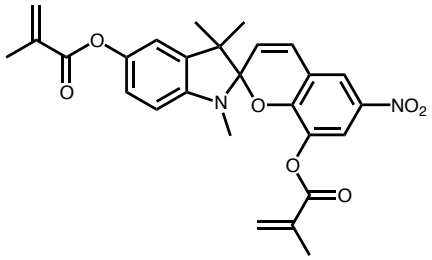

Figure 4.8. Diacrylate-functionalized mechanophore.

4.3.2 Methods

The solubility of the diacrylate-spiropryan is very low in most solvents and the high temperatures at which the polymerization occurs further limits the choice of possible solvents. In addition, NIPAM has a relatively low melting temperature (60-63°C). This allowed a melt polymerization procedure to be used in which molten NIPAM was the reaction solvent. Recrystallized NIPAM (1.091 g, 9.64 mmol), diacrylate-spiropyran (2.1 mg, 4.4×10^{-3} mmol), and AIBN (2.5 mg, 0.0152 mmol) were combined in a 7-mL vial with a magnetic stirbar. Only a small amount of crosslinker (0.05 mol%) was used in the initial experiments in an effort not to waste material, as it requires a significant amount of time to synthesize. The vial was placed in an oil bath at 70°C and stirring was allowed to continue for 15 minutes, at which point the stirbar was removed. The vial was purged with nitrogen for 5 minutes, and the reaction was allowed to continue for 3 hours.

4.3.3 Results

After 3 hours, the vial containing the solid, dark red polymer was removed from the oil bath (**Figure 4.9**). The SP-NIPAM polymer, much like SP-HEMA, was recovered by breaking the glass vial and removing any glass fragments. A small section of the gel was removed (Figure 4.9b) and added to H_2O in a scintillation vial to swell the gel and remove any unreacted monomer. However, the crosslinker density was very low and the speed in which the reaction occurred apparently did not allow for the mechanophore to diffuse through the molten NIPAM. As a result, the majority of the non-crosslinked polymer chains dissolved in the water and only a small amount remained insoluble (Figure 4.9c).

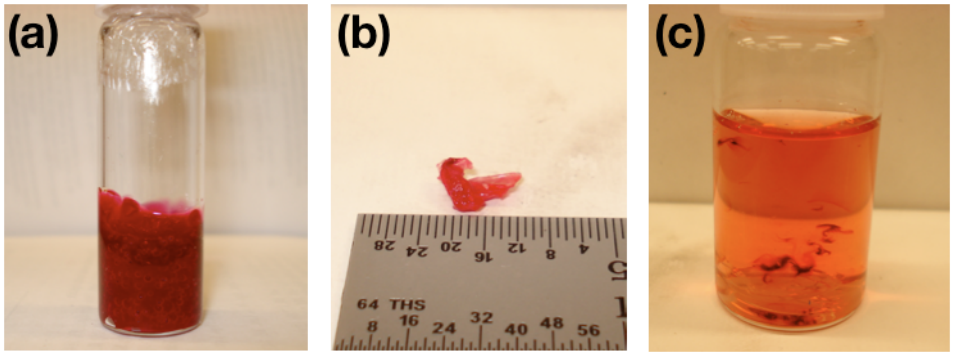

Figure 4.9. (a) SP-NIPAM gel after polymerization and (b) small section of SP-NIPAM. (c) Vial containing part (b) section in H_2O after 24 hours.

As with the SP-HEMA, the mechanophore in SP-NIPAM was thermally activated during synthesis. The hydrogel was placed under the microscope and exposed to high intensity visible light to revert the mechanophore back to the nonpolar spiropyran form. After a few minutes, the entire gel sample was a light brown color, indicating the mechanophore was in the spiropyran form. After the light was extinguished, the polymer reverted back to the colored form, much like

the SP-HEMA. However, the transition time was much longer, indicating the polar form of the mechanophore wasn't as strongly preferred in the less polar NIPAM (**Figure 4.10**).

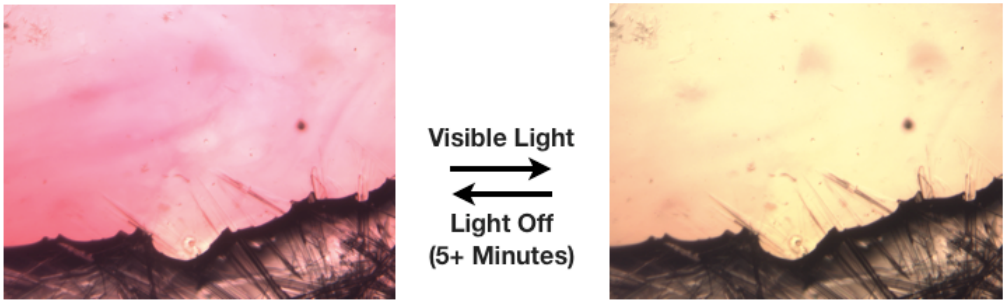

Figure 4.10. Photo-switching of mechanophore in SP-NIPAM polymer. After removal of light source, mechanophore reverts back to polar merocyanine form.

4.4 Spiropyran-PMMA Hydrogels

Traditional hydrogel polymers proved to be too polar to allow the spiropyran mechanophore to be incorporated and have it remain in its nonpolar form. Therefore, the transition was made to nontraditional, and more nonpolar, hydrogels. Poly(methyl methacrylate), or PMMA, is a glassy, hydrophobic polymer that has been investigated with mechanical activation in spiropyran.[9, 10] PMMA has also been used the as the major component of hydrogel materials.[11-14] The hydrophobicity of the polymer is overcome by the inclusion of a hydrophilic segment to form a copolymer.

4.4.1 Materials

The previously mentioned diacrylate-spiropyran was again used as the mechanophore crosslinker. Methyl methacrylate (MMA) and AIBN were obtained from Sigma Aldrich. Prior to use, methyl methacrylate monomer was filtered through a plug of basic alumina to remove the inhibitor. Dichloromethane was purchased from Fisher and used as received.

4.4.2 Methods

Diacrylate-SP (17.2 mg, 0.0359 mmol) was added to a 20-mL scintillation vial containing MMA (6.62 g, 66.1 mmol) and AIBN (10.1 mg, 0.0615 mmol). The vial was covered with a septum, and the solution was mixed using a vortex mixer. After the components were in solution, the vial was purged with nitrogen for 5 minutes then placed in an oven at 70°C for 24 hours. As with the previous NIPAM synthesis, only 0.05 mol% SP was used in an effort to save material.

4.4.3 Results

The polymer product was recovered by breaking the vial and, unlike the HEMA and NIPAM products, the polymer and vial separated very easily. **Figure 4.11** shows synthesized SP-PMMA, and the mechanophore was again thermally activated by the elevated temperatures during synthesis. The polymer was swollen with an excess of dichloromethane to remove any unreacted components (**Figure 4.12**). At room temperature, the polymer is too glassy to easily switch between the spiropyran and merocyanine forms, so the dichloromethane also acted as a plasticizer and small pieces of the polymer were removed with a razor blade. Some of the plasticized pieces were allowed to dry (deplasticize) at ambient conditions while others were air-dried under illumination from a high intensity visible light (Figure 4.12b). Once the polymer pieces were completely deplasticized, the particular form of the mechanophore in each piece was "frozen" in the glassy polymer. The pieces that were allowed to dry in ambient conditions therefore remained in the polar merocyanine form while those dried under intense visible light illumination remained in the nonpolar spiropyran form (Figure 4.12c). However, the SP-PMMA

polymers, in both merocyanine and spiropyran forms, were still much too hydrophobic to exhibit the desired mechanically induced swelling behavior.

Figure 4.11. Two sections of SP-PMMA after removal from synthesis vial.

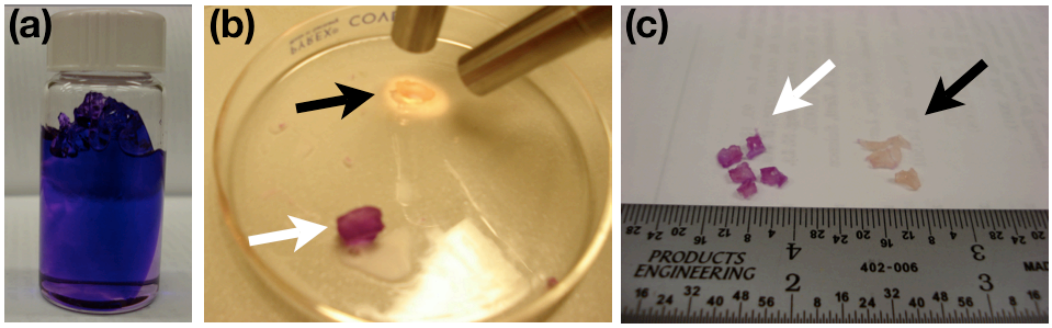

4.12. (a) Section of SP-PMMA in dichloromethane. (b) Two pieces of SP-PMMA in Petri dish drying under high intensity visible light (black arrow) and drying under ambient conditions (white arrow). (c) Multiple pieces of SP-PMMA after drying under high intensity visible light (black arrow) and ambient conditions (white arrow).

4.5 P(MMA:NIPAM) and P(MMA:HEMA) Copolymers

HEMA and NIPAM were initially chosen as the copolymers in SP-P(MMA:copolymer) experiments since their behavior with the spiropyran crosslinker was already well understood. It was hypothesized that the correct balance of hydrophobic/hydrophilic interactions could be achieved by varying the monomer ratios of HEMA or NIPAM and MMA. Initial copolymer synthesis and swelling experiments were performed using divinylbenzene (Sigma Aldrich)

instead of the spiropyran crosslinker since only the overall swelling profiles of the copolymers were of interest. However, preliminary P(MMA:NIPAM) syntheses resulted in products that were heavily phase-separated. This resulted in glassy PMMA segments that did not swell and hydrophilic NIPAM segments that swelled significantly in Millipore H_2O (**Figure 4.13**).

In contrast, the P(MMA:HEMA) copolymers were not phase-separated but they absorbed the same amount of water as pure PMMA (around 3 wt-%) until reaching a critical HEMA concentration between 70 and 80% (**Figure 4.14**). At these significant HEMA percentages, the polymer no longer behaved as a glassy solid, and the nonpolar form of the mechanophore could not be trapped within the gel after drying (i.e. polar merocyanine form was again preferred) (**Figure 4.15**).

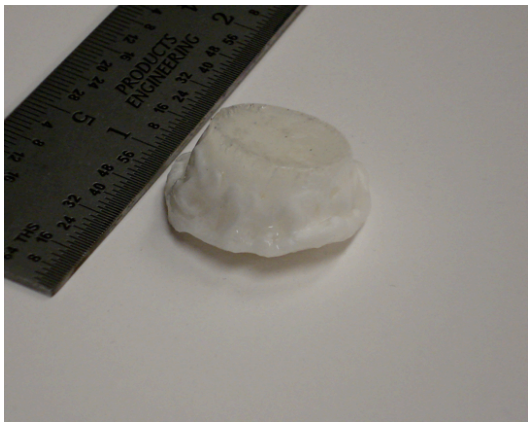

Figure 4.13. Phase-separated P(MMA:NIPAM) copolymer after 48 hours in H_2O. Glassy PMMA section (top) and swelled NIPAM section (bottom).

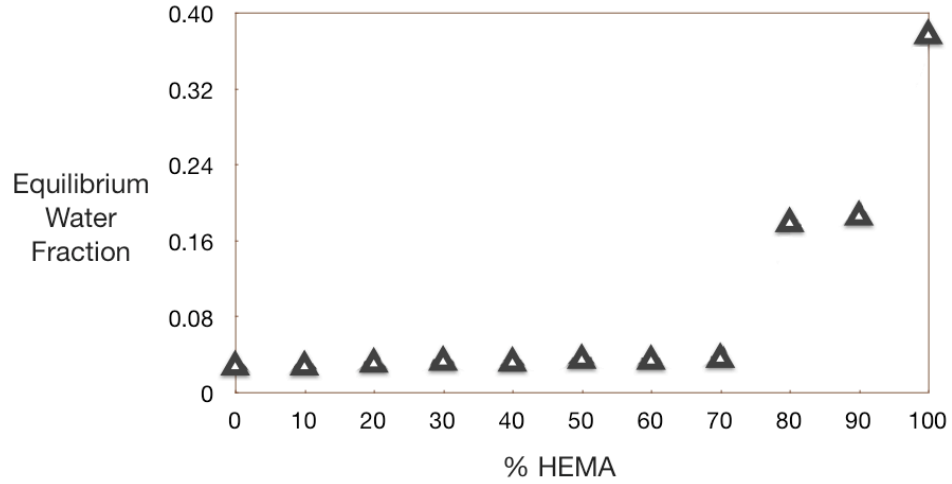

Figure 4.14. Swelling profile of P(MMA:HEMA) copolymers. EWF (equilibrium water fraction) is calculated as EWF = (Ws – Wd)/Ws where Ws and Wd are the fully swollen and dry weights, respectively. EWF holds to that of pure PMMA (~0.03) until reaching a critical HEMA concentration between 70 and 80%.

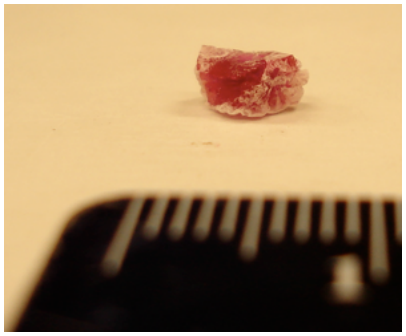

Figure 4.15. SP-P(MMA:HEMA) (3:7) after swelling and drying under high intensity visible light. The nonpolar form of the mechanophore could not be trapped in the copolymers with high HEMA ratios.

4.6 Summary

Spiropyran was incorporated as a crosslinker into a number of different polymeric systems. The mechanophore was originally incorporated into HEMA and NIPAM, traditional hydrogel polymers. The initial crosslinking strategy used urethane linkages and the easily synthesized dihydroxyspiropyran to attach to the HEMA backbone. However, functionalization proved difficult and the diacrylate-spiropyran was used for the remainder of the experiments. Nevertheless, both HEMA and NIPAM proved too polar to allow for the nonpolar form of the mechanophore to be preferred within the hydrogel. Nonpolar PMMA hydrogels were then

investigated and the glassy nature of the polymer allowed both the nonpolar spiropyran and polar merocyanine forms to be trapped. PMMA-copolymers were then prepared in an attempt to increase the hydrophilicity of the polymer while still maintaining its glassy character. However, P(MMA:NIPAM) experienced significant phase-separation problems while P(MMA:HEMA) required such a large percentage of HEMA that the glassy character was lost and the nonpolar form of the mechanophore could not be trapped.

4.7 References

1. Qiu, Y.; Park, K., *Advanced Drug Delivery Reviews* **2001,** *53* (3), 321-339.

2. Samanta, S.; Locklin, J., *Langmuir* **2008,** *24* (17), 9558-9565.

3. Vlassiouk, I.; Park, C.-D.; Vail, S. A.; Gust, D.; Smirnov, S., *Nano Letters* **2006,** *6* (5), 1013-1017.

4. Benito-Lopez, F.; Byrne, R.; Raduta, A. M.; Vrana, N. E.; McGuinness, G.; Diamond, D., *Lab on a Chip* **2009,** *10* (2), 195-201.

5. Lee, C. K.; Davis, D. A.; White, S. R.; Moore, J. S.; Sottos, N. R.; Braun, P. V., *Journal of the American Chemical Society* **2010,** *132* (45), 16107-16111.

6. Aronhime, M.; Einstein, K.; Cohn, D., *Clinical Materials* **1994,** *15* (3), 161-167.

7. Cohn, D.; Aronhime, M.; Abdo, B., *Journal of Macromolecular Science, Part A* **1992,** *29* (10), 841-851.

8. Senshu, K.; Yamashita, S.; Mori, H.; Ito, M.; Hirao, A.; Nakahama, S., *Langmuir* **1999,** *15* (5), 1754-1762.

9. Davis, D. A.; Hamilton, A.; Yang, J.; Cremar, L. D.; Van Gough, D.; Potisek, S. L.; Ong, M. T.; Braun, P. V.; Martinez, T. J.; White, S. R.; Moore, J. S.; Sottos, N. R., *Nature* **2009,** *459* (7243), 68-72.

10. Beiermann, B. A.; Davis, D. A.; Kramer, S. L. B.; Moore, J. S.; Sottos, N. R.; White, S. R., *Journal of Materials Chemistry* **2011,** *21* (23), 8443-8447.

11. Cornejo-Bravo, J. M.; Arias-Sanchez, V.; Alvarez-Anguiano, A.; Siegel, R. A., *Journal of Controlled Release* **1995,** *33* (2), 223-229.

12. Siegel, R. A.; Firestone, B. A., *Macromolecules* **1988,** *21* (11), 3254-3259.

13. Swann, J. M. G.; Bras, W.; Topham, P. D.; Howse, J. R.; Ryan, A. J., *Langmuir* **2010,** *26* (12), 10191-10197.

14. Varshosaz, J.; Falamarzian, M., *European Journal of Pharmaceutics and Biopharmaceutics* **2001,** *51* (3), 235-240.

CHAPTER FIVE

CONCLUSIONS AND FUTURE WORK

5.1 Electrospinning of Spiropyran-Polyurethane

5.1.1 Determination of Molecular Orientation Within SP-PU Nanofibers

As discussed in the introductory chapter, electrospinning has been shown to produce nanofibers with increased molecular orientation.[1-3] As a result, it was assumed that orientation was also present in SP-PU, but this was not confirmed. Pedicini *et al*.[4] used linearly polarized FTIR to determine the degree of orientation within non-mechanophore-containing polyurethanes, and this technique should be suitable for SP-PU since the mechanophore is present in such low concentrations. The optics to perform such experiments were purchased and initial orientation experiments were attempted, but time did not permit a comprehensive study. Before any additional mechanical activation experiments are performed, orientation studies need to be completed to determine the actual degree of molecular alignment.

5.1.2 Use of a Different Adhesive to Prevent Fiber Slippage

In an attempt to prevent nanofiber slipping within the fiber bundles, Loctite® 495 superglue was used to "grab" each end of multiple nanofibers. However, the small diameter of the aligned bundles, and the very small gauge length allowed the superglue to wick across the bundle. The fiber bundle diameter and gauge length will be very difficult to change, although a more viscous glue might reduce wetting across the bundle. There are more gel-like versions of superglue manufactured by Loctite®, but the highly exothermic polymerization of the

cyanoacrylate-based glue might plasticize the nearby polyurethane nanofibers and destroy any molecular orientation introduced by electrospinning.

5.1.3 Single-Nanofiber Mechanical Testing

As discussed previously, there has been significant work on single-nanofiber mechanical tests, some of it performed by the Ioannis Chasiotis group here at the University of Illinois.[5] It is possible these MEMS devices could be used for the testing of a SP-PU single fiber or a group of SP-PU single fibers. The primary difficulty to this approach would be the detection of spiropyran activation. Even the most sensitive fluorescence detection would probably be too insensitive to detect activation within a single nanofiber since there is such a small amount of mechanophore present. Therefore, the highest probability of success is most likely through the use of a group of several nanofibers. This may require the development of a new testing procedure by the Chasiotis group although it might be plausible through a collaboration.

5.2 Electrospinning of *gem*-Dibromocyclopropane Mechanophores

5.2.1 gDBC Auto-Activation and NMR Detection Limit

Brett Beiermann, a fellow member of the Autonomic Materials Systems group at the Beckman Institute, also experimented with the same batch of *g*DBC polymers that were used for the electrospinning tests. He attempted to achieve mechanical activation of bulk *g*DBC polymer under a number of conditions, including high heat, tensile loading, and compressive stresses. However, no activation of the mechanophore was detected, making it likely the sample that was received was either inherently unreactive or had experienced some other type of auto-activation during the shipping process. Furthermore, in work later published, Lenhardt and coworkers[6]

were able to achieve bulk tensile activation of *g*DBC polymers, but this activation was substantially less than that of compressive stresses and was near the limit of detection of NMR. Thus, any future studies of *g*DBC activation by electrospinning might require the production of substantial amounts of nanofibers, something that has not been possible thus far.

5.2.2 Lower Molecular Weight gDBC Sample

The highest molecular weight *g*DBC polymer available (300 kDa) was initially chosen since longer polymer chains are exposed to greater mechanical stresses during the electrospinning process.[7] However, a molecular weight of this magnitude resulted in solubility problems and solution inhomogeneities, which resulted in difficulties during electrospinning. The use of a lower molecular weight *g*DBC polymer, perhaps between 100 and 200 kDa, might alleviate some of the solubility issues and allow for more consistent, maintained electrospinning.

5.3 Multi-Functional Spiropyran-Containing Hydrogels

As discussed previously, glassy hydrogels have been realized by the preparation of a copolymer containing a hydrophilic monomer and MMA.[8-10] The particular hydrophilic monomer chosen was 2-(dimethylamino)ethyl methacrylate, or DMAEMA. In addition to being inherently hydrophilic, this monomer acquires a positive charge at acidic pH, making it even more hydrophilic (**Figure 5.1**). In addition to varying the monomer ratios, this added pH-functionality could allow a finer level of tuning in regards to the hydrophilic-hydrophobic balance within a SP-P(MMA:DMAEMA) gel. Preliminary experiments included the synthesis of a divinylbenzene-crosslinked P(MMA:DMAEMA) (7:3 mol ratio) gel, which resulted in clear, glassy copolymer samples. One piece of the gel was placed in Millipore H_2O while another was

placed in 1 M HCl (**Figure 5.2**). Over the course of a week, the sample in acidic solution experienced an increase of 44-wt% while the sample in pure water increased by only 3-wt%, a value typical for pure PMMA. These results were promising but time did not permit further investigation. Future experiments should include the incorporation of spiropyran crosslinker and swelling tests to determine if the nonpolar form of the mechanophore can be trapped in the glassy copolymer.

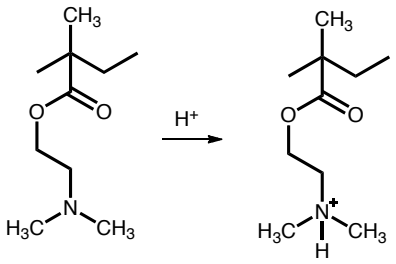

Figure 5.1. Protonation of DMAEMA monomer under acidic conditions. Protonation results in a dramatic increase in hydrophilicity.

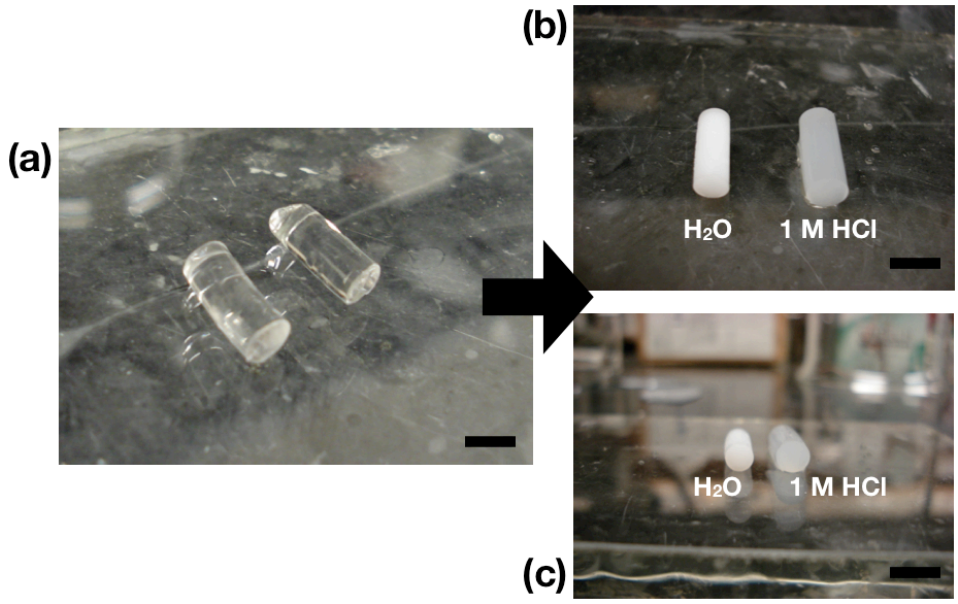

Figure 5.2. (a) 2 identical P(MMA:DMAEMA) polymer sections after synthesis. (b) Sections from (a) after 1 week in respective solution and (c) axial view of copolymer samples. Sample in H_2O experienced ~3-wt% increase while sample in acidic solution increased by 44-wt% (scale bars = 1 cm).

5.4 References

1. Fennessey, S. F.; Farris, R. J., *Polymer* **2004,** *45* (12), 4217-4225.

2. Yee, W. A.; Kotaki, M.; Liu, Y.; Lu, X., *Polymer* **2007,** *48* (2), 512-521.

3. Kakade, M. V.; Givens, S.; Gardner, K.; Lee, K. H.; Chase, D. B.; Rabolt, J. F., *Journal of the American Chemical Society* **2007,** *129* (10), 2777-2782.

4. Pedicini, A.; Farris, R. J., *Polymer* **2003,** *44* (22), 6857-6862.

5. Naraghi, M.; Chasiotis, I.; Kahn, H.; Wen, Y.; Dzenis, Y., *Appl. Phys. Lett.* **2007,** *91*, 151901.

6. Lenhardt, J. M.; Black, A. L.; Beiermann, B. A.; Steinberg, B. D.; Rahman, F.; Samborski, T.; Elsakr, J.; Moore, J. S.; Sottos, N. R.; Craig, S. L., *Journal of Materials Chemistry* **2011,** *21* (23), 8454-8459.

7. Bellan, L. M.; Cross, J. D.; Strychalski, E. A.; Moran-Mirabal, J.; Craighead, H. G., *Nano Lett* **2006,** *6* (11), 2526-30.

8. Cornejo-Bravo, J. M.; Arias-Sanchez, V.; Alvarez-Anguiano, A.; Siegel, R. A., *Journal of Controlled Release* **1995,** *33* (2), 223-229.

9. Siegel, R. A.; Firestone, B. A., *Macromolecules* **1988,** *21* (11), 3254-3259.

10. Varshosaz, J.; Falamarzian, M., *European Journal of Pharmaceutics and Biopharmaceutics* **2001,** *51* (3), 235-240.